CHAPTER 8

SURVEY OF EXPERIMENTAL RESULTS

Philippe Cardin & Daniel Brito

8.1. INTRODUCTION

Liquid metals in magnetohydrodynamics experiments and fluids in motion self–sustaining natural dynamos share a common property, a very low magnetic Prandtl number (Pm), the ratio of kinematic viscosity to magnetic diffusivity. Pm of liquid metals in the core of terrestrial planets are indeed very small ($< 10^{-4}$) although being in extreme pressure and temperature conditions (Chapters 4 & 5 and Poirier, 1988). In gaseous planets, the hydrogen gas presents a metallic phase at large pressure (Chapter 5 and Guillot, 1999) with again a low Pm . The plasma of convective regions of stars (Chapter 6) and diluted gas in magnetospheres also have low Pm . Small Pm for liquid metals as well make us believe that most of natural dynamos may be modeled and studied in a laboratory. Many groups in the world have focused their liquid experiments on fundamental aspects of the magnetohydrodynamics of natural objects.

So far, two experiments in Riga (Latvia) and in Karlsruhe (Germany) have succeeded in observing dynamo action in an experiment, using liquid sodium. Sodium was chosen mainly because it is the highest conductor of electricity among other liquid metals at laboratory conditions. With liquid sodium, it is possible to reach magnetic Reynolds number ($\mathrm{Rm} = UL/\eta$) of a few tenths in an experiment of metric size, where U is the typical velocity of the fluid, L is the typical scale of

the experiment and η the magnetic diffusivity (see Table VI for numerical values), the velocity and size being chosen to optimize Rm. Note however that the velocity of a fluid inside a container of a given size is directly related to the mechanical power available to run the experiment. In a turbulent regime, the power P may be expressed as the cubic power of the velocity

$$P \approx \rho L^2 U^3 \,, \tag{8.1}$$

where ρ is the density of the fluid, as measured for example in the Riga experiment (see Section 8.3.6 and Figure 8.15). In presence of global rotation or other external forcing, a different scaling of the power (Cardin *et al.*, 2002) may be obtained but lead to the same conclusion: a huge power of a few hundreds of kilowatts has to be injected in a metric size experiment of sodium in order to reach Rm larger of order 100. That explains why dynamo experiments require generally heavy infrastructures.

Like every other liquid metals, liquid sodium has a very low magnetic and thermal Prandtl numbers (see Table VI) showing that magnetic diffusion is much larger than thermal diffusion, thermal diffusion being also much larger than viscous diffusion. It is worth to note that the magnetic diffusion time $\tau_\eta \propto L^2/\eta$ of an experimental dynamo of metric size of liquid sodium is order of a few seconds, a very long time compared to the dynamical time (overturn time for a fluid particle below $10^{-1}\,\mathrm{s}$ in a metric size dynamo experiment). It means that the observation of a growing magnetic field for more than a few seconds during an experiment would be the demonstration of dynamo action and that experiments running for thousand diffusing magnetic times are, in principle, feasible.

The intrinsic molecular properties of liquid metals makes numerical simulations of magnetohydrodynamics dynamos very difficult. From the low Pr and Pm numbers for liquid metals, one expects indeed that temporal and spatial scales of the magnetic field, first, the velocity field, second, and the temperature field, third, to be very different. As $\mathrm{Rm} = \mathrm{RePm}$, dynamo experiments with large Rm of a few tens will have a very large hydrodynamic Reynolds number Re ($\approx 10^7 - 10^8$), meaning that experimental dynamos will have undoubtedly strong turbulent flows. In presence of a strong magnetic field or rotation, the statistical and geometrical properties of these turbulent magnetohydrodynamics flows may be possibly different from the ones of pure hydrodynamical turbulence: in the Earth's core for example (Chapter 4) the Reynolds number is presumably very high ($\mathrm{Re} \gg 1$), but the non-linear term in the Navier-Stokes equation is of second order compared to Coriolis and Lorentz forces (Ro = Inertial term/Coriolis forces $\ll 1$, N = Lorentz forces/Inertial term $\gg 1$) and therefore the non-linear chaotic behaviour of the system might be induced by the non-linear term in the induction equation or the non-linear term in the energy equation.

The fluid flow expected in dynamos being turbulent, it could be of interest to use

turbulent diffusivities to describe small scales in numerical modelisation (Glatzmaier & Roberts, 1995; Matsushima *et al.*, 1999; Philipps *et al.*, 2003; Buffett, 2003). However, little is known about these processes in magnetohydrodynamics cases and experiments are certainly needed to check the validity of these concepts and to propose scaling laws for turbulent diffusivities (see Section 8.3.9). More generally, experiments are oftentimes very precious because they enable the verification of theoretical considerations or the confirmation of numerical calculations. They can also test the validity of assumptions necessary to understand the physics of dynamos. A great advantage of experiments compared to numerical simulations is that experiments are run with real metallic fluids with known physical properties, these ones could not be adjusted as a parameter like in numerical simulations. The experiments shed light also on new unexpected effects and new unexpected regimes. The drawbacks of experiments are the measurements which are generally limited, in particular for the ones in the bulk of the fluid where the dynamo process operates: experiments require an important theoretical and numerical work to complete the understanding of measurements. Note that experiments with liquid metals can also lead to improvements in technology and instrumentation which may indirectly benefit to the industry of metallurgy, as an example.

From a mathematical point of view, a dynamo exists when a non zero magnetic field is solution to the equation [induction equation (1.14), Chapter 1]. Clearly, $\mathbf{B} = \mathbf{0}$ is also solution. In the laboratory, it is very difficult to have a strictly zero external magnetic field around the experiment. The magnetic field of the Earth itself produces an ambient magnetic field of few tenths of Gauss ($1 - 5 \times 10^{-4}\,\mathrm{T}$, see Chapter 4). From a theoretical point of view, it is very difficult to differentiate a self–sustained magnetic field of an experimental dynamo from the one produced by a simple amplification of the ambient field by the velocity flow. The same problem exists regarding the observation of planetary magnetic fields; for instance, the magnetic field of Io is believed to be produced by magnetoconvection in the core of Io in presence of the jovian external magnetic field (Sarson *et al.*, 1997). In practice, during an experiment, one is convinced to observe a self–induced magnetic field by looking first at the amplitude of the magnetic field compared to the ambient field, and second at the time duration of the observation compared to the magnetic diffusion time. Moreover, there is generally a very clear transition as you vary your experimental parameters between the induction and the self–induction of a magnetic field.

Many experiments aimed to model dynamics of astrophysical and geophysical dynamos have been realised but let us restrict this review to experiments directly devoted to the understanding of the dynamo action. Other experiments on thermal convection in a rotating sphere, on precession, on boundary effects or instabilities, on magnetohydrodynamics turbulence that have been carried out to understand the basic dynamics on which a dynamo can start are reported in a review by Nataf (2003).

Table VI - Liquid sodium properties at $393\,^{\circ}\mathrm{K}$ ($120\,^{\circ}\mathrm{C}$).

Density	ρ	932×10^3	$\mathrm{kg\,m^{-3}}$
Dynamic viscosity	μ	6.2×10^{-4}	$\mathrm{kg\,m^{-1}\,s^{-1}}$
Kinematic viscosity	$\nu \equiv \mu/\rho$	6.77×10^{-7}	$\mathrm{m^2\,s^{-1}}$
Fusion temperature	T_f	97.8	$^{\circ}\mathrm{C}$
Thermal expansion coefficient (at $298\,^{\circ}\mathrm{K}$)	α	7.1×10^{-5}	$^{\circ}\mathrm{K}^{-1}$
Thermal conductivity	k	85.9	$\mathrm{W\,^{\circ}K^{-1}\,m^{-1}}$
Specific heat	C	1373	$\mathrm{J\ kg^{-1}\,^{\circ}K^{-1}}$
Thermal diffusivity	$\kappa \equiv k/(\rho\, C)$	6.71×10^{-5}	$\mathrm{m^2\,s^{-1}}$
Electrical conductivity	σ	9.35×10^6	$\Omega^{-1}\,\mathrm{m^{-1}}$
Magnetic diffusivity	$\eta \equiv (\mu_0\,\sigma)^{-1}$	8.53×10^{-2}	$\mathrm{m^2\,s^{-1}}$
Prandtl number	$\mathrm{Pr} \equiv \nu/\kappa$	10^{-2}	
Magnetic Prandtl number	$\mathrm{Pm} \equiv \nu/\eta$	7.9×10^{-6}	

This chapter will be divided in two parts. The first part describes a set of experiments where the same definition of dimensionless numbers is used throughout, in order to make easier comparison between experiments. It ends with a discussion on sodium technology and measurements. The experimental results are discussed in terms of dynamo mechanisms in the second part. Future challenges of experimental dynamo modeling are exposed in the conclusion.

8.2. DESCRIPTION OF THE EXPERIMENTS

A survey of magnetohydrodynamics experiments devoted to study high magnetic Reynolds numbers flows is presented here in a chronological order. Although numerous experiments greatly improved our knowledge on dynamo mechanisms until 1999, that year can be considered as a turning point since the dynamo effect was, for the first time, measured in a flow of liquid sodium, quasi-simultaneously in Riga (Gailitis *et al.*, 2000) and Karlsruhe (Müller & Stieglitz, 2000). In parallel to these two successful dynamo experiments, a number of high magnetic Reynolds experiments of second generation have been quite recently run in order to look for amplification of the magnetic field by a flow less constrained than in Riga or Karlsruhe. Some new projects of sodium experiments are presented at the end of this survey. In the following, every experiment is described and presented in a schematic diagram and completed by a table giving its main characteristics and relevant dimensionless numbers.

Specific conditions linked to the utilisation of sodium in dynamo experiments are listed at the end of this section. Progress and limitations of measurement techniques in dynamo experiments are eventually discussed.

8.2.1. A RAPIDLY ROTATING DISC IN A CYLINDER OF SODIUM

B. Lehnert might be considered as a pioneer of magnetohydodynamics experiments with liquid metals such as mercury (Lehnert, 1951; Lehnert & Little, 1956) and sodium (Lehnert, 1958). Its most relevant experiment for dynamo mechanisms is the latter one performed in liquid sodium. He constructed a cylindrical vessel filled with sodium, a rotating copper disk driving the flow inside. Lehnert successfully verified the so-called ω–effect by measuring the conversion of an imposed poloidal magnetic field $\mathbf{B}_0$ (generated by a coil below the vessel) into a toroidal one by an axisymmetric flow of liquid sodium.

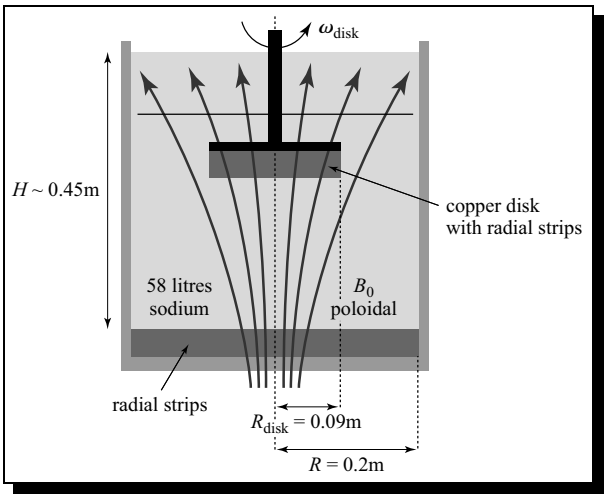

▷ Power of the rotating motor, $P_{\rm motor} \leq 3\,{\rm kW}$.
▷ $\omega_{\rm disk} \leq 500\,{\rm rpm}$ (rounds per minute).
▷ $B_0 \leq 0.03\,{\rm T}$ at the height of the disk.
Measurements:
▷ Power input for a constant rotation rate of the motor.
▷ Induced magnetic field measured by a probe coil in the bulk of the fluid.

▷ ${\rm N} = \dfrac{\sigma B_0^2\, R}{\rho\,(\omega_{\rm disk} R_{\rm disk})} \simeq 0 - 1.$

▷ ${\rm Rm} = \mu_0 \sigma (\omega_{\rm disk} R_{\rm disk}) R \leq 10.$

▷ Prediction: induced field of the same order of the imposed magnetic field with the same apparatus if $\rightarrow \omega_{\rm disk} \simeq 3000\,{\rm rpm}$.

8.2.2. A DYNAMO WITH TWO SOLID ROTATING CYLINDERS

Lowes & Wilkinson (1963, 1968) achieved in a laboratory the first solid dynamo experiments following an idea of Herzenberg (1958). Two ferromagnetic cylinders of iron alloy with their axes at right angle were rotated independently in a housing of the same material (Lowes & Wilkinson, 1963). Electrical contacts between the housing and the rotating cylinders were done with liquid mercury. With adequate directions of rotation and sufficiently high angular velocities for the cylinders, a seed ambient magnetic field was amplified and eventually, at the critical Rm, the magnetic field of the system (cylinder 1 and cylinder 2) became self–sustained provided the cylinders were kept rotating at the same velocities. The dynamo mechanism was the following: the induced toroidal magnetic field (via an ω–effect, see Section 8.3.1) of cylinder 1 provides the external poloidal magnetic field of cylinder 2, the induced toroidal magnetic field (ω–effect also) of cylinder 2 providing in turn the external poloidal magnetic field of cylinder 1. Note that with a slightly modified experimental set-up, still with ferromagnetic materials, Lowes & Wilkinson (1968) could even witness reversals of the self–sustained magnetic field in their system.

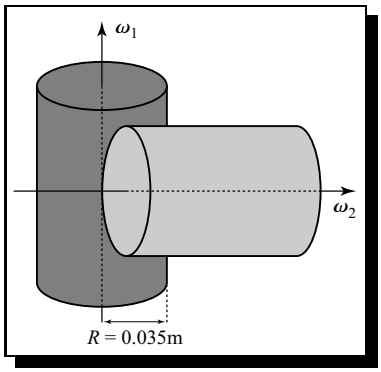

▷ $P_{\mathrm{motor}} \approx 2 \times 100\,\mathrm{W}$.
▷ $\omega_1 \simeq \omega_2 \leq$ $2000 - 3000\,\mathrm{rpm}$.
▷ $B_0 =$ ambiant magnetic field.
▷ $\mu_{\mathrm{iron\ alloy}} \simeq 150\mu_0$.
▷ Depth between the two axes of the cylinder $= 0.08\,\mathrm{m}$ in the 1963 experiment.

Measurements:
▷ Induced magnetic field.
▷ Differences in electrical potential between cylinders.
▷ $B_{\mathrm{induced}} \leq 0.1$T.
▷ $\mathrm{Rm} = \mu^*_{\mathrm{iron}}\sigma\omega R^2 \leq 200$.

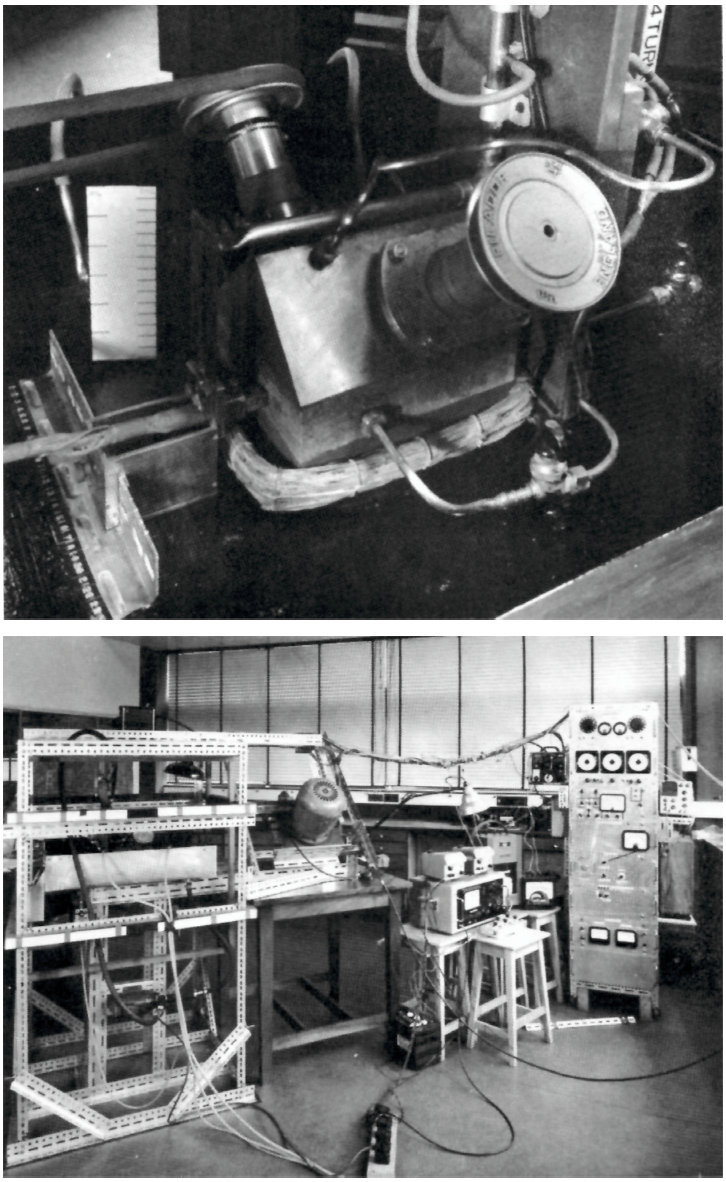

Figure 8.1 - The experiment of F. Lowes and I. Wilkinson at Newcastle in 1963 (courtesy F. Lowes).

8.2.3. THE α–BOX EXPERIMENT

A joint Postdam-Riga experiment was constructed to measure the so called α-effect in a small modulus: liquid sodium was run through a system of orthogonally wounded channels of stainless steels (Steenbeck *et al.*, 1968). The set-up was designed to drive the sodium through an helicoidal flow under an imposed magnetic field. Differences in electrical potential between the bottom and the top of the modulus were measured with a pair of electrodes in the direction of the imposed magnetic field.

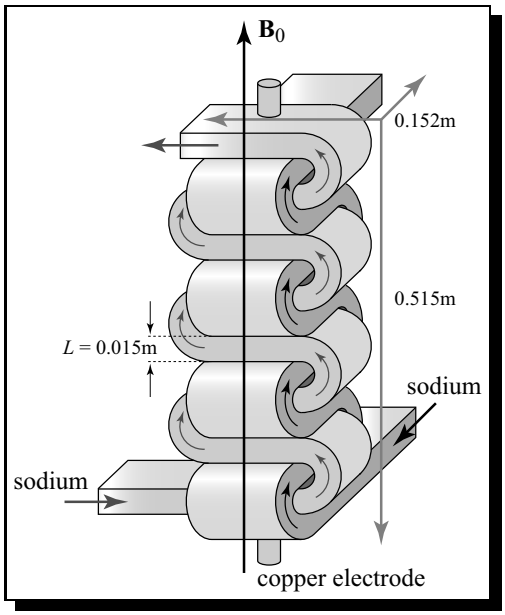

▷ Number of horizontal channels along the total height = 28.
▷ Sodium velocity, $U_{\max} = 11\,\mathrm{m\,s^{-1}}$.
▷ $B_0 \leq 0.3\,\mathrm{T}$.
Measurements:
▷ Differences in electrical potential between the top and bottom with electrodes.

▷ $\mathrm{Re} = \dfrac{UL}{\nu} \simeq 5 \times 10^5$.

▷ $\mathrm{N} = \dfrac{\sigma B_0^2 L}{\rho U} \simeq 0 - -30$.

▷ $\mathrm{Rm} = \mu_0\, \sigma\, U\, L \leq 2$.

8.2.4. A PRECESSING EXPERIMENT IN LIQUID SODIUM

Gans (1970) initiated the magnetohydrodynamics experiments in presence of a global rotation of the system (in presence of the Coriolis force): he built a precessing experiment in liquid sodium following the work of Malkus (1968) in water. A cylinder filled with liquid sodium was rotating with an axisymmetric imposed magnetic field along its rotation axis. All the set-up was spun-up simultaneously on a rotating table, at right angle of the rotation axis of the cylinder. The experiment was built with the theoretical idea that the precession of the Earth's core may be one of the main source of energy of the dynamo (Malkus, 1993; Kerswell, 1996; Noir *et al.*, 2003). Unfortunately, due to technical difficulties, Gans (1970) could not run the experiments in the full parameter regime.

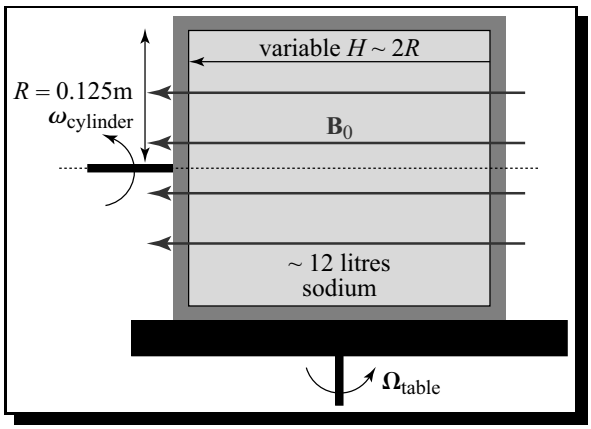

▷ $\omega_{\text{cyl}} \leq 3600\,\text{rpm}$.

▷ $\Omega_{\text{tab}} \leq 50\,\text{rpm}$.

▷ $B_0 = 0.023,\ 0.046\,\text{T}$ by a d.c. coil.

Measurements:

▷ Torque imposed by the rotation of the cylinder induced magnetic field.

▷ $\text{E} = \dfrac{\nu}{\Omega_{\text{tab}} R^2} \simeq 10^{-7}$.

▷ $\text{N}\ \dfrac{\sigma B_0^2 R}{\rho(\omega_{\text{cyl}} R)} \simeq 10^{-2}$.

▷ $\text{Rm} = \mu_0\ \sigma\ \omega_{\text{cyl}}\ R^2 \leq 70$.

8.2.5. THE FIRST PONOMARENKO TYPE EXPERIMENT

Upon a theoretical prediction of dynamo action in a endless helical stream of screw type (Ponomarenko, 1973; see also Chapter 1, Section 1.6.1) for a relatively low critical magnetic Reynolds, an experimental set up was assembled in Riga and run in Leningrad in 1986 (Gailitis *et al.*, 1987). More than 150 litres of sodium was powered by electromagnetic pumps and circulated through a cylinder with an helicoidal diverter at the top. The external field was imposed by a 3–phase generator as theoretically required by the Ponomarenko dynamo. Although the experiment was run successfully, it had to be stopped probably close to the dynamo onset (see Section 8.3.5 and Figure 8.11) due to mechanical vibrations in the central thin wall of stainless steel in the center of the modulus.

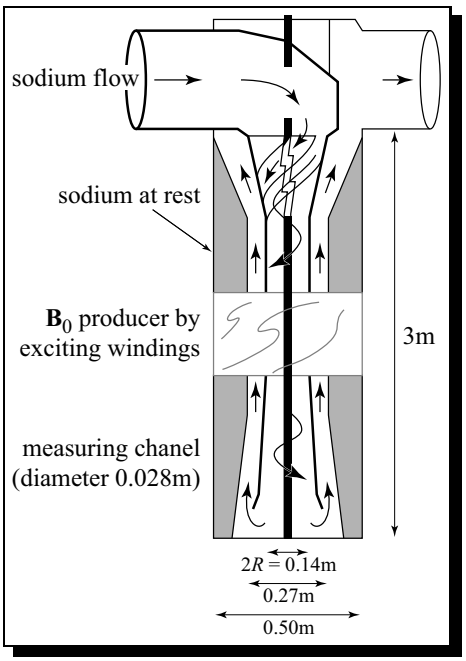

▷ $T_{\text{experiment}} \simeq 200^o\text{C}$.
▷ Flow Sodium rates
$Q_{\text{sodium}} 280 - 660\,\text{m}^3\,\text{h}^{-1}$.

Measurements:
▷ Sodium flow rate (electromagnetic flow meter).
▷ Induced magnetic field inside the channel.

▷ $U_{\max} = \dfrac{Q_{\max}}{\pi R^2} \simeq 12\,\text{m}\,\text{s}^{-1}$.

▷ $\text{Rm} = \mu_0\,\sigma\,U\,R\,\leq 8$.

8.2.6. THE VORTICES OF GALLIUM

In the mid-ninety's two experiments were run using liquid gallium. Gallium has a low point of fusion (30^oC), is a fairly high conductor of electricity (3 times larger than mercury, but 3 times smaller than sodium), and is easier and safer to handle in a laboratory compared to sodium or mercury.
Motivated to describe a geophysical relevant regime where Lorentz and Coriolis forces are comparable in magnitude, Brito *et al.* (1995, 1996) run an isolated vortex generated by a rotating disk at the bottom, the vortex being also rotated on a table (to add the Coriolis force to the flow). A transverse magnetic field was imposed perpendicular to the axis of rotation. A set of measurements was performed: gallium velocity inside the vortex, differences in electrical potential at the vortex boundary, induced magnetic field outside the vortex and gallium temperature. These measurements accompanied by a numerical model of the electrical current circulation in the bulk of the vortex allowed to describe quantitatively the dynamics of that geostrophic vortex under the presence of a transverse imposed magnetic field. Brito *et al.* (1996) derive a quantitative scaling law of the Joule dissipation as a function of the forcing and the imposed magnetic field.

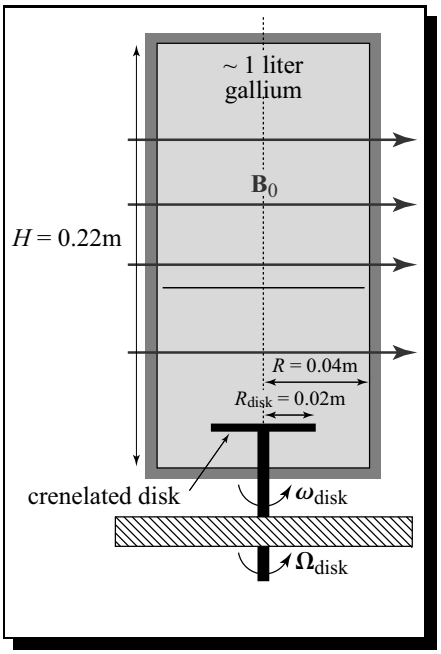

▷ $P_{\rm motor} = 1.3\,{\rm kW}$.
▷ $\omega_{\rm disk} \leq 3000\,{\rm rpm}$.
▷ $\Omega_{\rm table} \leq 90\,{\rm rpm}$.
▷ $B_0 \leq 0.075\,{\rm T}$.
Measurements:
▷ Gallium velocity field (Venturi tubes at the top).
▷ Induced magnetic field (Hall probe).
▷ Differences in electrical potential (copper electrodes).
▷ Gallium temperature (thermistor).
▷ Torque applied by the rotating motor.

▷ $\displaystyle {\rm Ro} = \frac{(\omega_{\rm disk} R_{\rm disk})}{\Omega_{\rm table}\, R} \simeq 0.7 - 15.$

▷ $\displaystyle {\rm N} = \frac{\sigma B_0^2\, R}{\rho\, (\omega_{\rm disk} R_{\rm disk})} \simeq 0 - 1.$

▷ $\displaystyle {\rm E} = \frac{\nu}{\Omega_{\rm table} R^2} \simeq 10^{-4} - 10^{-6}.$

▷ $\displaystyle \Lambda = \frac{\sigma B_0^2}{\rho \Omega_{\rm table}} \simeq 10^{-3} - 1.5.$

▷ ${\rm Rm} = \mu_0 \sigma (\omega_{\rm disk} R_{\rm disk}) R \leq 0.1.$

Odier *et al.* (1998, 2000) generated the so-called Von Kármán flow in gallium in a cylinder with two corotating disk in presence of an imposed magnetic field parallel or orthogonal to the vertical axis of the cylinder. Measurements of the magnetic field inside the cylinder allowed to describe precisely the advection and expulsion of the imposed magnetic field.

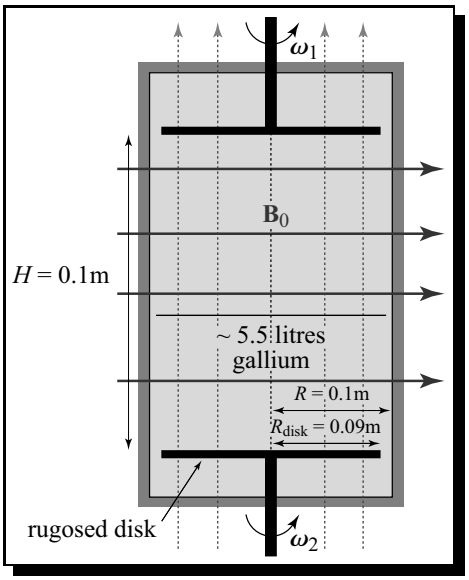

▷ $P_{\rm motor} = 2 \times 11\,{\rm kW}$.
▷ $\omega_{\rm disk} \leq 3000\,{\rm rpm}$.
▷ $B_0 \leq 0.002\,{\rm T}$.
Measurements:
▷ Induced magnetic field at various depth in the equator plane (Hall probes)
▷ Dynamic pressure at the cylinder boundary (piezoelectric transducer).

▷ ${\rm N} = \dfrac{\sigma B_0^2\, R}{\rho\,(\omega_{\rm disk} R_{\rm disk})} \simeq 0 - 10^{-4}$.

▷ ${\rm Re} = \dfrac{(\omega_{\rm disk} R_{\rm disk}) R}{\nu} \leq 10^8$.

▷ ${\rm Rm} = \mu_0 \sigma \omega_{\rm disk} R_{\rm disk} R \leq 3$.

8.2.7. THE RIGA DYNAMO

After the promising results of the Leningrad experiment (see Section 8.2.5), the latvian team built a new experimental modulus: the shape and sizes of the central channel were changed, an important effort was done to optimize the velocity profiles both with experiments in water and numerical modelisation (Stefani *et al.*, 1999; see Section 8.3.5). The shape of the propeller was also optimised and eventually, the main change was the replacement of the electromagnetic pumps by two powerful motors driving the propeller at the top of the modulus (Gailitis *et al.*, 2002).

The first experimental evidence of dynamo action was obtained in Riga at the end of the year 1999 (Gailitis *et al.*, 2000): an imposed field as close as possible to the expected one by the Ponomarenko dynamo theory was amplified during an experiment, as measured by flux gate-sensors along the vertical of the modulus. The dynamo magnetic field spatial distribution and frequency were studied as a function of the rotation rate of the propeller above the critical magnetic Reynolds number. Saturation of the self–sustained magnetic field was observed (Gailitis *et al.*, 2001).

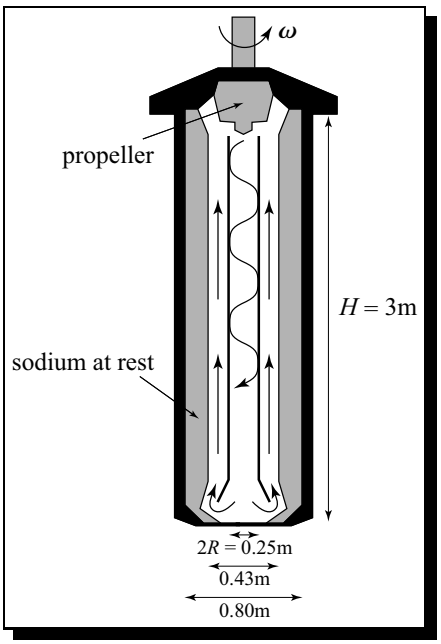

▷ $P_{\rm motor} \leq 120\,{\rm kW}$.
▷ $\omega \leq 2200\,{\rm rpm}$.
▷ B_0 is an helicoidal field along the vertical axis of the modulus.

Measurements:
▷ Induced magnetic field with flux gates and Hall sensor at different heights along the vertical.
▷ Motor power delivered as a function of rotation rate.
▷ Monitoring of the sodium temperature.

▷ ${\rm Rm} = \mu_0 \sigma \omega R^2 \leq 42$.

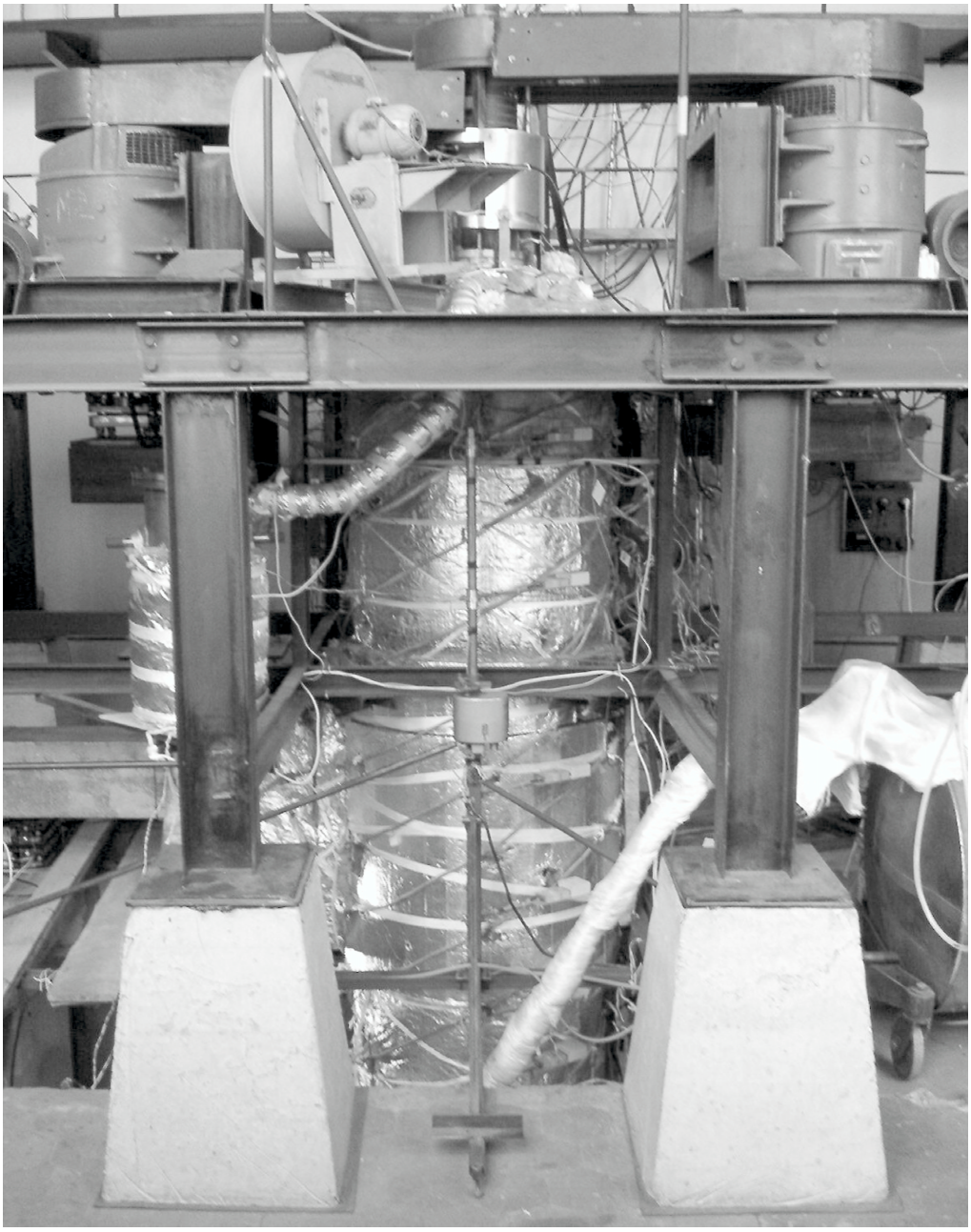

Figure 8.2 - The Riga dynamo experiment (photograph courtesy F. Stefani).

8.2.8. THE KARLSRUHE DYNAMO

The self–excitation was also observed in Karlsruhe in a device based on a theoretical two-scale periodic kinematic dynamo of G.O. Roberts (1972), see Section 1.5. It was designed jointly by Busse (Bayreuth) and Müller (Karlsruhe) (Busse *et al.*, 1996). A set of 52 spin-generators were assembled in a large modulus, a pair of spin-generators being distinctively shown in the figure (Müller & Stieglitz, 2000). Each generator contains a central tube where the sodium is flowing unidirectionnaly with a flow rate V_C and an outer part where the sodium flows with an helicoidal forced motion with a flow rate V_H. The sodium is going up (sign +) and down (sign -) in his neighbouring generator. The gap between the 52 helicoidal cylinders is filled with liquid sodium at rest. Three electromagnetic pumps forced the sodium to flow in and out of the modulus, one pump running the sodium through the central tubes, and the two other ones through the helicoidal outer part. Sodium flow rates were monitored. Beyond the critical rate for both flows (central and outer part), magnetic measurements showed that the ambient magnetic field was rapidly amplified and saturated after a transient time (Stieglitz & Müller, 2001; Müller *et al.*, 2004).

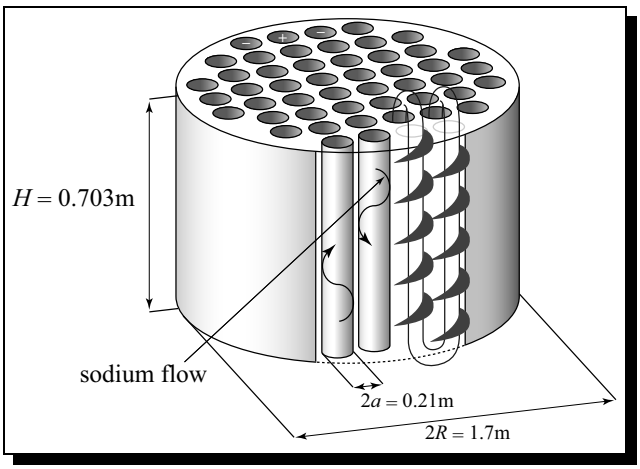

▷ Flow sodium rates $Q_{\rm sodium}\ 70 - 120\,{\rm m}^3\,{\rm h}^{-1}$.
▷ $P_{\rm threepumps} \leq 500\,{\rm kW}$.
▷ B_0 ambient magnetic field.

Measurements:
▷ Induced magnetic field (three components) at various locations inside and outside the modulus (Hall probes).
▷ Induced magnetic field with compass needles outside the modulus.
▷ Flow rates of sodium.
▷ Sodium temperature.

▷ $U_{\rm max} = Q_{\rm sodiummax}/(\pi a^2) \simeq 1\,{\rm m\,s}^{-1}$
▷ ${\rm Rm} = \mu_0 \sigma U_{\rm max} R^2 \leq 10$

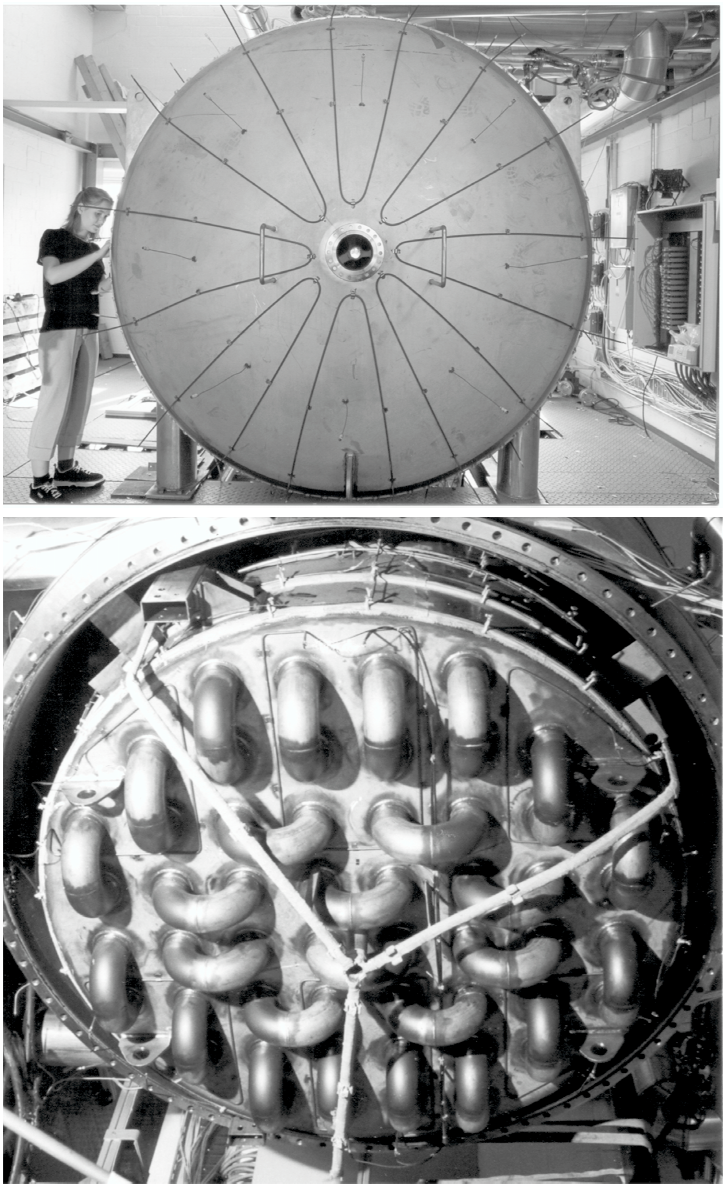

Figure 8.3 - The Karlsruhe dynamo experiment (courtesy U. Müller, R. Stieglitz).

8.2.9. THE COLLEGE PARK EXPERIMENTS

The group of D. Lathrop have been running sodium experiments for a few years in College Park, Maryland. They have performed convective experiments (Peffley *et al.*, 2000a; Shew *et al.*, 2002), as well as mechanically forced magnetohydrodynamics flow (Peffley *et al.*, 2000b; Sisan *et al.*, 2003). This mechanically forced spherical experiment is motivated by kinematic dynamo calculations of Dudley & James (1989) which predict a critical magnetic Reynolds number possibly reachable in a laboratory with the following type of flow used by Lathrop and collaborators: two mixing propellers drive the flow in a sphere filled with sodium (co or counter rotating propellers). Baffles attached to the outer boundary are added to the rotating sphere in order to increase the vigour of the mixing. An imposed magnetic field is either parallel (dashed lines) or orthogonal (solid lines) to the rotating shaft. That team have been using a pulse decay measurements of an externally applied field to quantify how far they were from the dynamo transition during an experiment (see Section 8.3.5). Trying to get closer to the dynamo transition, they have tried number of various set-up by changing for example the shape of the propeller or by changing boundary conditions adding equatorial copper discs at the equator of the sphere (Shew *et al.*, 2001).

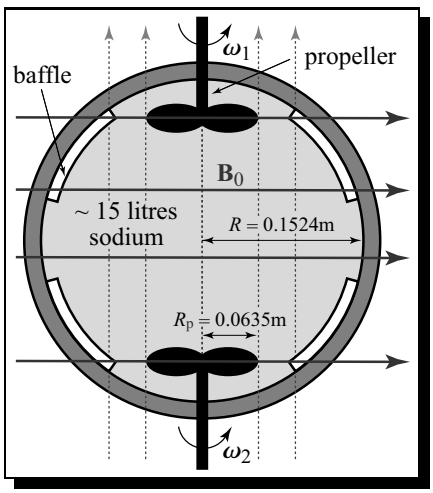

▷ $P_{\rm motor} \leq 15\,{\rm kW}$.
▷$\omega_1 \simeq \omega_2 \leq 3000\,{\rm rpm}$.
▷$B_0 \leq 0.2\,{\rm T}$.
Measurements:
▷ Induced magnetic field after imposed pulses, measured by Hall probes.
▷ Mechanical power as a function of rotation rate.
▷ Monitoring of the sodium temperature.

▷ $N = \dfrac{\sigma B_0^2\, R}{\rho \omega R_p} \simeq 0 - 17.$
▷ ${\rm Rm} = \mu_0 \sigma \omega R_p R \leq 30.$

8.2.10. VON KÁRMÁN SODIUM EXPERIMENTS

The Von Kármán Sodium or VKS experiments performed in Cadarache (France) are aimed to pursuit the Von Kármán Gallium (see Section 8.2.6) experiments at higher magnetic Reynolds number (Bourgoin *et al.*, 2002; Marié *et al.*, 2002). Again, the VKS flow is of type Dudley & James (1989) with a possible relatively low critical magnetic Reynolds number. That team has put a lot of energy to calibrate the VKS experiments on one hand experimentally, in water and in gallium with similar set-ups, and in the other hand numerically, by using kinematic dynamo calculations based on velocity flows measured in water (Bourgoin *et al.*, 2002; Marié *et al.*, 2002; Marié *et al.*, 2003) (see Section 8.3.5). They looked in particular at the optimised ratio of poloidal versus toroidal field velocity for the dynamo action. They have observed so far an amplification of the imposed the imposed magnetic field but not reached a self–sustained magnetic field regime (Bourgoin *et al.*, 2002; Pétrélis *et al.*, 2003).

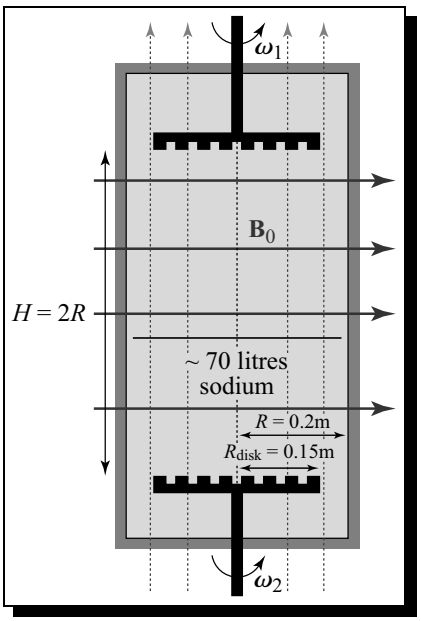

▷ $P_{\rm motor} = 2 \times 75\,{\rm kW}$.
▷ $\omega_{\rm disk} \leq 1500\,{\rm rpm}$.
▷ $B_0 \leq 0.002\,{\rm T}$.

Measurements:
▷ Induced magnetic field inside the flow using a 3D Hall probe.
▷ Dynamic pressure at the wall.
▷ LDV velocity measurements in water experiments.

▷ ${\rm Rm} = \mu_0 \sigma \omega_{\rm disk} R_{\rm disk} R \leq 50$

8.2.11. DERVICHE TOURNEUR SODIUM PROJECT

The Geodynamo team (Grenoble, France) has constructed an experiment devoted to study the magnetostrophic regime in a sphere (experiment called DTS or Derviche Tourneur Sodium), that is when the Lorentz and Coriolis forces are dominant in the flow. An inner and an outer sphere can rotate independently, and the magnetized inner sphere carry an imposed dipolar magnetic field (Cardin *et al.*, 2002). The particularity of this project lies in the crucial *rôle* of Coriolis or rotational forces, presumably very important in the generation of most planetary magnetic fields (Chapters 4 & 5).
Experiments in water with a similar geometry for the experimental set-up are presently run and compared to direct numerical simulation (Schaeffer & Cardin, 2005); present results indicate that such a spherical-Couette flow might be favorable for dynamo action. The dynamo regime is not expected in the present experimental set-up as DTS is rather small in size.

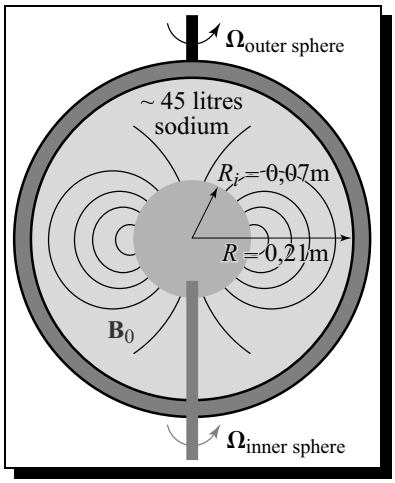

▷$P_{\text{motor}} = 2 \times 11\,\text{kW}$.
▷$\Omega_{\text{in}} = \Omega_{\text{out}} \leq \pm 3000\,\text{rpm}$.
▷$B_0 = \leq 0.022\,\text{T}$ at mid-depth of the shell.
Measurements:
▷ Ultrasonic Doppler velocimetry for the sodium flow.
▷ Induced magnetic field outside the shell.
▷ Differences in electrical potential at the outer sphere boundary.

▷ $\text{E} = \dfrac{\nu}{\Omega_{\text{out}} R^2} \simeq 10^{-8}$.

▷ $\Lambda = \dfrac{\sigma B_0^2}{\rho \Omega_{\text{out}}} \leq 0.2$.

▷ $\text{Rm} = \mu\sigma(\Omega_i - \Omega_o (R - R_i/2))R \leq 20$.

8.2.12. THE MADISON PROJECT

C. Forest and collaborators in Madison, Wisconsin, have been preparing an experimental dynamo also based on a Dudley & James type flow in a sphere (Forest *et al.*, 2002). The experiment is close to the geometry of the experiment of Lathrop's group but larger in size. That group has put a lot of emphasis on the hydrodynamic experimental modelisation of the flow, in particular to select the most appropriate propeller to drive a flow as close as possible to the Dudley & James one. Velocity measurements performed in water were used in a kinematic dynamo model to predict that the present size of the experiment and the power of the motors should drive an homogeneous dynamo in sodium.

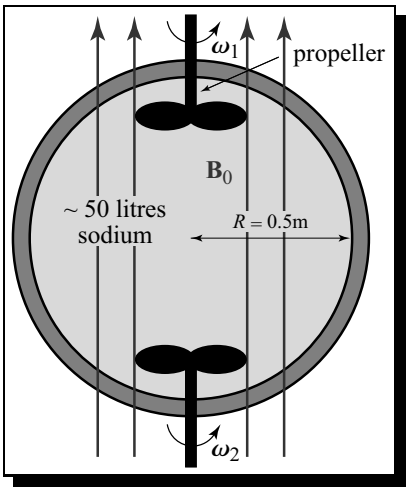

▷ $P_{\rm motor} \leq 2 \times 75\,{\rm kW}$.
▷ $U_{\rm max\ ,predicted} = 20\,{\rm m\,s^{-1}}$.
▷ $B_0 \leq 0.012\,{\rm T}$ via two coils.
▷ $60\,{\rm kW}$ of resistive heating elements.
▷ $35\,{\rm kW}$ of oil based heating/cooling.

Measurements:
▷ Laser Doppler velocimetery in the analogous experiment in water.
▷ Poloidal induced magnetic field with an array of 64 Hall probes at the surface of the sphere.
▷ Toroidal induced magnetic field with external toroidal coils?
▷ ${\rm N} = \dfrac{\sigma B_0^2 R}{\rho U} \simeq 0 - 1.$
▷ ${\rm Rm} = \mu_0 \sigma U_{\rm max} R \leq 12$.

8.2.13. THE PERM PROJECT

A new kind of experimental dynamo project is under study in Perm, Russia. That project relies also on the Ponomarenko dynamo, more specifically on dynamo action caused by a strongly time-dependent helical flow. The idea is to used a toroidal channel filled with liquid sodium ($\simeq 100\,{\rm litres}$) with an helicoidal diverter inside (Frick *et al.*, 2002). The torus would be accelerated to a very high velocity of rotation of order 3000 rounds per minute (rpm) and then stopped abruptly. The dynamo effect should then observed during the spin-down time of the torus. Experiments in water and kinematic calculations are promising for the dynamo experiment (Frick *et al.*, 2002; Dobler *et al.*, 2003): the dynamo in such a torus requires a short time of braking of less than 0.2 second. A thin and very high conductive shell is required for the torus (copper) and an appropriate seed magnetic field could be assembled with an arrangement of permanent magnets around the torus.

8.2.14. THE SOCORRO PROJECT

A dynamo experiment is under development in Socorro, New-Mexico, around the group of S. Colgate to create an $\alpha\omega$ type experiment. The experiment uses a Taylor Couette flow between two cylinders rotating at different angular velocities to model the ω–effect (Colgate *et al.*, 2002). The α–effect is produced by the rising of two jets of liquid sodium at the base of the experiment. Experiments in water and kinematic dynamo calculations are currently performed and indicate that self–excitation of a magnetic field might be reachable in such an experimental device.

8.2.15. A NEW PRECESSING PROJECT IN SODIUM

Following the experiments of Gans (1970), the group of J. Léorat is at present studying a cylindrical precessing experiment type flow, in Meudon, France. A preliminary experiment in water as well as numerical kinematic calculations (Léorat *et al.*, 2001) would constrain the dynamics of the precessing flow in a cylinder at a high hydrodynamical Reynolds number as well as the power dissipated by such a flow. That water project being achieved, a sodium experiment with a large cylinder of metric size precessing would follow.

8.2.16. TECHNOLOGY AND MEASUREMENTS IN DYNAMO EXPERIMENTS

LIQUID SODIUM AND ITS PROPERTIES

As seen throughout the survey of experiments, liquid sodium is now broadly used in high magnetic Reynolds experiments and appears to be the preferred working fluid to model dynamos in a laboratory. Its main physical properties are shown in Table VI. As mentioned in the introduction, its electrical conductivity is very large [see Nataf (2003) for comparison of physical properties of gallium and mercury] but also its low density and melting point makes it very attractive to use in a laboratory. The large production of sodium ($23000\,\mathrm{tons\,yr^{-1}}$ in France for example) makes it quite inexpensive (10 euros/kg for sodium) compare to other metals ($1000\,\mathrm{euros/kg}$ for gallium for example). The main difficulty to handle sodium is its strong reactivity with water, air and plenty of other materials such as alcohol, concrete, etc... As an example, sodium reduces water with production of hydrogen which may spontaneously explodes in air. At high temperature ($\geq 250^o\mathrm{C}$), droplets of sodium may even burn in air with small flames generating solid oxydes at the surface of liquid sodium or aerosol in the surrounding atmosphere. That explains why dynamo experiments are run usually in installations dedicated to nuclear technology with a high

degree of knowledge of sodium handling (Forschungszentrum Karlsruhe GmbH, Karlsruhe experiment; Institute of Physics, Salaspils, Riga experiment; Cadarache, Comissariat l'energie atomique, VKS experiment) or in particular buildings without any water just devoted to run sodium experiments (Grenoble for example).

EXTRACTION OF POWER AND SEALING

As seen in the introduction, a large amount of power must be introduced in dynamo experimental set-ups. The power is ultimately converted in heat through viscous or magnetic dissipation. If the heat is not extracted, the temperature of sodium rises quickly decreasing the Rm (because the electrical resistivity of sodium increases with temperature) and the experiments are run for a limited time of order a minute like in Riga or Cadarache. The experiment is then kept at rest for a few minutes or hours until the sodium cools down generally to around $120^o\mathrm{C}$. In Karlsruhe, the circulation of sodium through powerful heat exchangers allowed them to run their experiments for a few hours without stopping; this kind of circulation of sodium through exchangers is also under development in a new experimental set-up of VKS. In Grenoble, in a smaller device where only $20\,\mathrm{kW}$ are injected, a strong flow of cool/hot circulation of air around the rotating sphere is planned to monitor the temperature of the experiment. Note also that an oil circulation extracting the heat around the container is also a possibility used for example in the Madison experiment.
Leakage of sodium in a dynamo experiment with a vigourous flow of sodium may be very damaging. However, dynamic sealings in sodium are not entirely satisfactory, they are still under development; instead for example, in the VKS experiment, small leakage of sodium is permitted, in College Park, the joint around the rotating shaft is replaced after every run. As another example, the first dynamo run in Riga (November 1999) had also to be stopped because of a leakage of sodium at the top of the modulus. Experiments where no specifics sealings are needed such as the Karlrsrhue dynamo or the precession experiments (Gans, 1970; Léorat *et al.*, 2001) are in that respect very appealing. In Grenoble an electromagnetic coupling has been tested successfully to rotate the inner sphere; this solution also avoids sealing in sodium and might be promising.

MEASUREMENTS

Quantitative measurements in classical fluid dynamic experiments are usually difficult; they become very challenging in magnetohydodynamics experiments in sodium, in particular because electromagnetic waves can not be used. The temperature of sodium between 120^oC and 200^oC is a severe constraint and prevents the utilisa-

tion of classical measurements systems. In the following are presented the classical measurements performed nowadays in dynamo experiments. Most of them need a very good electronic system to process measured signals, protection from electromagnetic noise, digitilisation for analysis on computers. Even if the quality of the measuring probes is important, data processing is crucial.

Induced magnetic field: The key measurement in a magnetohydrodynamic experiment is the magnetic field. It is systematically measured in experiments. These measurements are usually done outside the flow. Indeed, despite the fact that local measurements in the flow may perturb the flow, magnetometer probes operate at low temperature and generally need a controled temperature tool to work properly. The probes are usually of two types: the Hall effect probes (B greater than a few microteslas) measure stationary and time varying (bandwith generally controled by the electronics) magnetic field. The principle of the second type of probes is based on the measurement of an induced electrical current produced by a time varying magnetic field in a coil (sensitivity and precision are directly connected to the coil and the electronics). Both measurements are unidirectionnal. These probes are generally small (less than a few milimeters). Given that a probe is one local measurement of one component of the magnetic field, it is very difficult to build a good spatial description of the magnetic field; an array of probes and is necessary in order to have a spatial description (see Forest *et al.*, 2002 for example). Note that large coils (size of the experiment) are used also to impose a magnetic field in the flow. The same coils may be used to measure the oscillating or vanishing induced magnetic fields.

Dynamic Pressure measurements: Dynamic pressures can be measured by piezoelectric probes at the contact with the fluid. Their typical sizes are a few milimeters of diameter. They can be very sensitive up to $1\,\mathrm{Pa}$. This technique measures time variations of the pressure (from a few Hz to a few tenths of kHz); they are used as indirect measurement of time variations of the velocity field. Pressure temporal spectra are then used to characterize the turbulence of the fluid flow.

Electrical potentials: Electrical potentials may be measured with copper electrodes in contact with the liquid sodium. The sensitivity and bandwith of these measurements are given by the ones of the measuring voltmeter. These potentials are difficult to interpret because they are related to the electrical currents which may have two sources, electrical or electromotive fields (Steenbeck *et al.*, 1968; see Section 8.2.3). The temporal evolution of the currents measured with electrodes at the edge of the container may be also directly related to the dynamic of the fluid flow (Brito *et al.*, 1995).

Fluid velocity measurements: The velocity field although being a key measurement in magnetohydrodynamic experiments is only very rarely measured mainly because sodium is opaque. Experimentalist use usually an indirect volumic measurement of the velocity field via the control of the torque (or power) delivered by rotating motors (Gailitis *et al.*, 2001, see Figure 8.15). Control of sodium flow rates through pumps also permits an averaged measurement of the velocity field, as in Karlsruhe for example (Stieglitz & Müller, 2001; e.g. Figure 8.16).
The intrusive hot film probes technique gives very good result in term of local variations of the velocity field. They are based on the measurement of the electrical resistivity of a conducting wire which vary with its averaged temperature which is controled by the flow around the wire. As far as we know, this technique has not been used in a dynamo experiment while it is largely used in MHD turbulence experiments (e.g. Alémany *et al.*, 1979).
A promising non intrusive technique to measure velocity fields in fluid dynamics experiment is the Doppler Ultrasound Velocimetry: it is based on the ultrasonic back scattering of oxydes (or other particles) in suspension in liquid sodium (for example). This technique successful in water, gallium, should work as well in sodium (Brito *et al.*, 2001; Eckert & Gerbeth, 2002). Laser Doppler velocimetry is also broadly used in experiments in water (Forest *et al.*, 2002; Marié *et al.*, 2003): water models of sodium experiments enable to measure the velocity field below the onset of the dynamo (see Section 8.3.5).

Temperature: Lastly, temperature measurements (usually also performed at the container boundaries) are easy to do. They are generally based on the measurement of the electrical resisitivity of a material which varies with the temperature. They may indicate the dissipation rate (or Joule dissipation) in the MHD flow (Brito *et al.*, 1996). Temperature probes can also be used to track the motion of thermal dynamic structures acting as passive tracers in front of temperature probes.

8.3. WHAT HAVE WE LEARNED FROM THE EXPERIMENTAL APPROACH?

In the second part of this chapter, results of the various experiments described in the first part are discussed altogether. Every section in the following is devoted to one particular aspect or related aspects of dynamo mechanisms. We will discuss up to what extent experiments validate or not the dynamo theory.

8.3.1. THE ω–EFFECT

A vortex of liquid metal permeated by an external magnetic field induces an azimuthal (toroidal) induced magnetic field parallel to the flow. This geometrical conversion of magnetic field lines is known as the ω–effect (Moffatt, 1978). Lehnert (1958, see Section 8.2.1) measured an induced azimuthal field up to 25% of the value of the initial imposed axial poloidal magnetic field. He produced a meridional map of the average induced field (Figure 8.4) with some singularities at the side boundary (reversed field) maybe due to singularities in the fluid flow. The same effect was measured by Brito *et al.* (1995) in a geostrophic vortex of liquid gallium (see Section 8.2.6) and quantitatively understood with loops of electrical currents and electrical potentials within the fluid flow: the transverse imposed magnetic field produced electrical Foucault currents parallel to the axis of the vortex, which in turn induced a magnetic field diffusing outside the tank where it was measured (Figure 8.5). The induced electrical currents were produced by shear layers as shown by the measurements and a numerical model in Brito *et al.* (1995); note that a solid body rotation would produce an ω–effect only in its periphery within the hydrodynamic shear boundary layer. This effect should instead be called the ω gradient effect to emphasize the importance of the differential rotation. These effects are clearly linear in Rm (Figure 8.5). More recently, the VKS experiments (8.2.10) in gallium and sodium also verified that mechanism for larger Rm (Odier *et al.*, 1998; Bourgoin *et al.*, 2002; Marié *et al.*, 2002; Figure 8.8).
Note that the Lowes & Wilkinson (1963) solid dynamo experiments (Section 8.2.2) relies upon the ω–effect also. Each solid cylinder transforms an axial component of the magnetic field into an azimuthal one; the position of both cylinders is chosen such that the azimuthal component of the magnetic field of a cylinder is axial to the other one. Electrical currents are produced at the periphery of the rotating cylinders in a thin layer of mercury which connects the main solid piece to the solid cylinder and loops in the solid parts creating an induced azimuthal field.

8.3.2. THE EXPULSION OF THE MAGNETIC FIELD

When the magnetic Reynolds number is high (Gubbins & Roberts, 1987) in a fluid flow, the magnetic field can be expelled from very active dynamical zones by the so-called process of expulsion of the magnetic field. This process may be understood as a skin effect: in the reference frame of the moving fluid (for example, a rotating frame at ω associated to a vortex of radius R), we consider a magnetic field which oscillates in time. The magnetic field penetrates the metal in a skin of size $\sqrt{\eta/\omega} = R/\sqrt{\mathrm{Rm}}$. Electrical currents are consequently produced in the skin layer which produced an induced magnetic field which is in the opposite direction of the imposed magnetic field in the heart of the vortex. The total magnetic field is then deflected

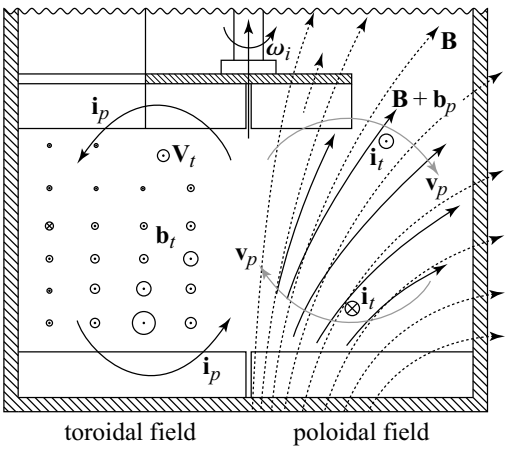

Figure 8.4 - Meridional map of the induced magnetic field demonstrating the ω–effect in the Lehnert's experiment (see Section 8.2.1). An imposed poloidal magnetic field B (dashed lines) is twisted into a toroidal magnetic field b_t (perpendicular arrows shown on the left, size of the circle proportionnal to b_t/B) by the toroidal velocity flow v_t. **i** stands for electrical currents. The resulting poloidal magnetic field lines $B + b_p$ (solid lines) seems to be expulsed (from Lehnert, 1958).

around the heart of the vortex. Lehnert (1958) (see Section 8.2.1) observed this effect in the poloidal part of the magnetic field as seen in Figure 8.4, in presence of the motion of the liquid sodium for $\mathrm{Rm} \gtrsim 5$), the magnetic field lines were deflected outside the sodium tank. Another evidence of this phenomena has been observed in the VKS experiment (see Section 8.2.10): at Rm above 30, there is a departure from the linearity associated to the ω–effect (Figure 8.6) and the induced magnetic field increases slower than predicted. In these cases, it is nevertheless difficult to differentiate the exact effect of the expulsion of the magnetic field from a dynamic change of the flow at high Rm. This second explanation, however, is unlikely since the interaction parameter N is rather small in both experiments. Note that the effect of a rotating magnetic field on a liquid metal flow has also been studied for its application in metallurgy (mixing techniques), these studies being generally focused on large interaction parameters (see Witkowski *et al.*, 1998, for example).

8.3.3. THE α–EFFECT

When there is production of an electrical current parallel to an imposed magnetic field, that process is called, in very general terms, the α–effect. Historically, this effect was introduced to model the effect of small scales on large scales in two scale

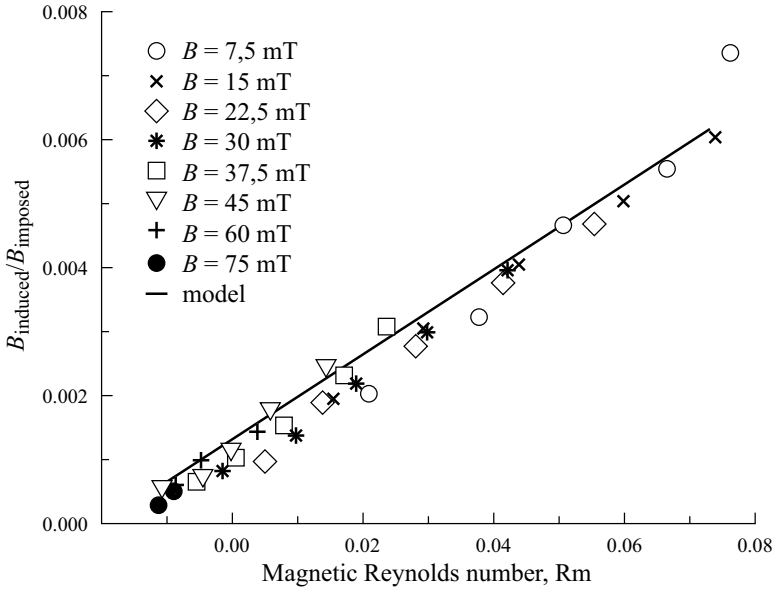

Figure 8.5 - Induced magnetic field B_{induced} by a vortex of gallium in an imposed magnetic field B_{imposed} (see Section 8.2.6). The ω–effect is a linear function of Rm(from Brito *et al.*, 1995).

dynamos as introduced in Section 1.5, but this effect can be generalised to the Parker effect for general flows (when two scales are not easy to determinate).
As soon as the α–effect was theoretically derived (Steenbeck *et al.*, 1966), the same team built the α–box (see Section 8.2.3) in order to prove the existence of this effect in the laboratory. Figure 8.7 from Steenbeck *et al.* (1968) shows that the measurements of differences in electrical potentials between the top and the bottom of the box are linear with the squared velocity and with the magnetic field as expected. However, it is not straightforward to interpret these electrical potential measurements as electrical currents: if a wire had been connected between the two electrodes, a back of the envelope calculation shows that a current of a few thousand amperes would have circulated between them (inducing a measurable magnetic field) if these electrical potentials were due to an average induced electrical current aligned with the imposed magnetic field in the volume of the α–box. Unfortunately, this type of measurements could not have been performed at that time and it is therefore possible that more complicated geometries of the currents inside the box (especially with the presence of stainless steel boundaries) were responsible of the measured electrical potentials. Nevertheless, the clear dependence in $|\mathbf{u}|^2$ is a strong proof of a second order effect in Rm, which is by definition an α–effect. Open questions remain however after that experiment: what would have been the measurements with

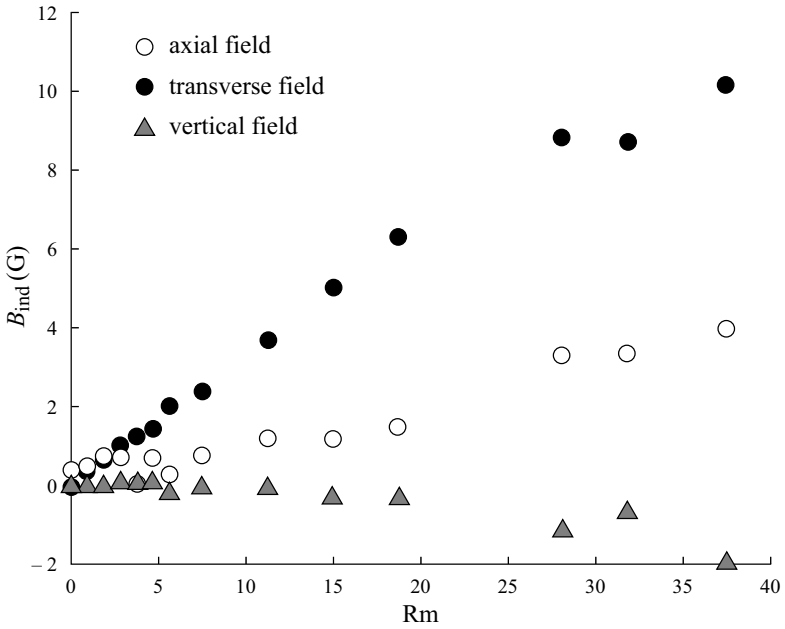

Figure 8.6 - Induced magnetic field $b_{\rm ind}$ measured in the VKS experiment (see Section 8.2.10) versus the magnetic Reynolds number Rm. An axial magnetic field (in direction of the axis rotation of the rotating disks) of $5.4 \times 10^{-4}\,\mathrm{T}$ is imposed. The linearity of the transverse (and azimuthal) component demonstrates the ω–effect and the departure from linearity may be associated to the expulsion of the magnetic field (from Marié *et al.*, 2002).

one cell instead of 28 (question regarding the scale separation), what was the *rôle* of helicity in the α–effect (as the flow in the pipe had not a proper helicity)?
A macroscopic α–effect has been seen in the VKS experiment (see Section 8.2.10). Pétrélis *et al.* (2003) measured an induced magnetic field perpendicular to the imposed magnetic field which is quadratic in Rm for small Rm as shown in Figure 8.8. Considering arguments of symmetry, they also showed that this magnetic field was associated to an electrical current parallel to the imposed magnetic field and that its sign was determined by the sign of the helicity. Although there was no clear scale separation in their experiment, their observation may be understood as a macroscopic α–effect or Parker effect.
The good agreement (see Section 8.3.6) between the experimental measurements in the Karlsruhe dynamo and the theoretical prediction of Rädler *et al.* (1998) using an α–effect in a mean-field approach (Chapter 1) is an indirect evidence of the presence of an α–effect in the Karlsruhe experiment (see Figure 8.16). There were unfortunetaly no direct measurements in the Karlsruhe apparatus which would have described

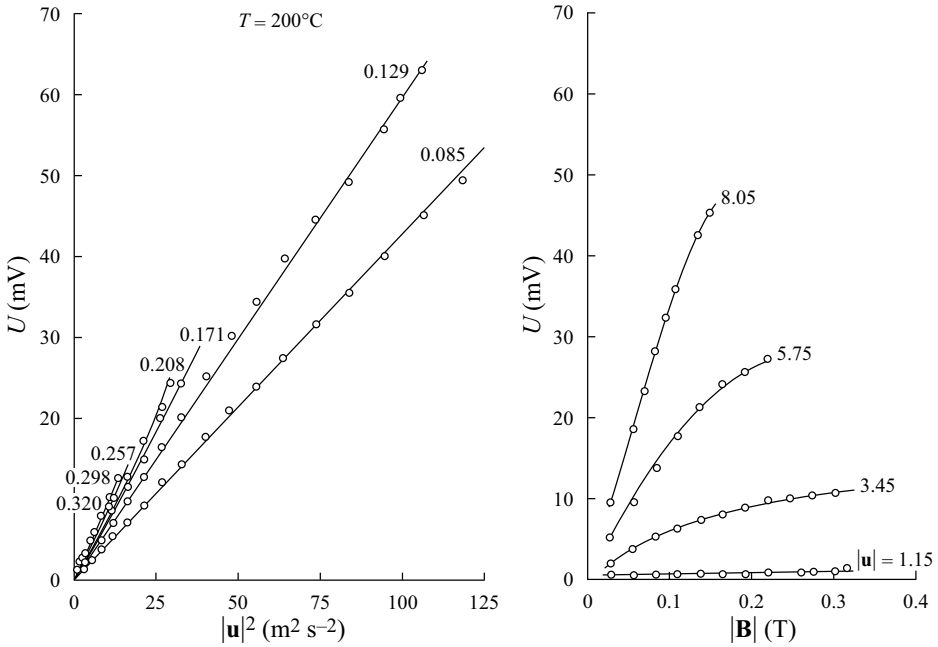

Figure 8.7 - (a) Differences in electrical potential measured in the α box (see Section 8.2.3) as function of the squared velocity ($\mathrm{m}^2\,\mathrm{s}^{-2}$) for different value of the imposed magnetic field (in T). (b) Differences in electrical potential measured in the α box as function of the imposed magnetic field for different value of the velocity (in m/s). The two linear dependances in $|\mathbf{B}_0|$ and $|\mathbf{u}|^2$ are the experimental proofs of the α–effect (from Steenbeck *et al.*, (1968).

in details the α–effect.

8.3.4. QUENCHING EFFECTS

In various experiments, linear and quadratic induction effects tends to saturate for large magnetic Reynolds number. This phenomenon is called the quenching effects (see Section 8.3.4). This effect is generally associated to the expulsion of the magnetic field from the moving part of the fluid (see Section 8.3.2) or with a change in the dynamic of the liquid metal generated by the Lorentz forces when the interaction parameter N is large. A clear evidence of a quenching effect can be seen in Figure 8.9 from Steenbeck *et al.* (1968). The electrical potentials decrease aproximatively as an hyperbola function of $|\mathbf{B}_0|^2$, the imposed magnetic field. One may conclude that the α–effect is reduced as the magnetic field increases.
A quenching effect can also be observed regarding the ω–effect. Figure 8.10 shows

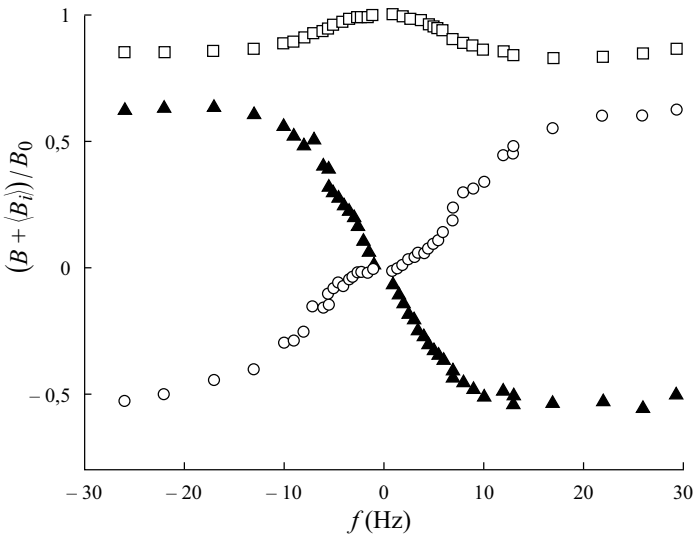

Figure 8.8 - Components of the total mean magnetic field as a function of the rotation frequency of a disk in the VKS experiment (see Section 8.2.10). The magnetic field B_0 is imposed along the y axis and the disk is rotating along the z axis. $(\circ)\langle B_x \rangle / B_0$; $(\square)(\langle B_y \rangle + B_0)/B_0$; $(\blacktriangle)\langle B_z \rangle / B_0$. For low rotation rates, B_z is linear with the velocity (ω–effect) while B_x shows a quadratic behaviour (second order induction effect or α–effect). Departures from this law are clearly seen for frequencies larger than $5\,\mathrm{Hz}$. This saturation may be seen as quenching effects (see Section 8.3.4) (from Pétrélis *et al.*, 2003).

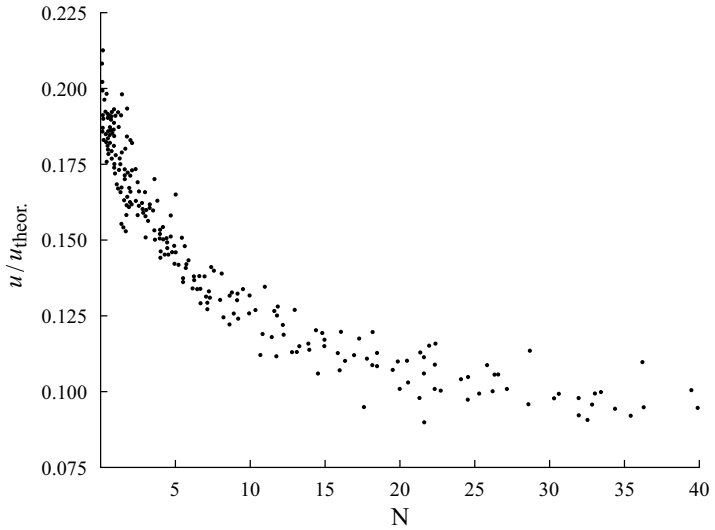

Figure 8.9 - Differences in electrical potential measured in all the experiments performed in the α–box (see Section 8.2.3) as function of the interaction parameter N. As a signature of the α quenching effect, the α–effect is reduced (hyperbolic decrease) when the magnetic field increases (from Steenbeck *et al.*, 1968).

the hyperbolic magnetic brake of a vortex by an imposed transverse magnetic field. In this case, it is really an effect of the magnetic field on the dynamic which explains this behaviour as the Rm is too low to have any expulsion of the magnetic field.
The departure from linear and quadratic variations of the components of the induced magnetic field for high rotation rate of the disk in the VKS experiment may be also interpreted in terms of quenching effects (see Figure 8.8).
The quenching effects reducing the efficiency of the α and ω–effect as the magnetic field grows, it may be seen as an important effect to saturate a self–induced magnetic field. More careful experimental analysis of these quenching effects are suited to better understand the saturation mechanism of dynamos.

8.3.5. THE EXPERIMENTAL KINEMATIC APPROACH OF THE DYNAMO

The kinematic approach means that you consider a stationary given flow (non affected by the Lorentz forces) and you measure its ability to induce a self–sustained magnetic field. If that approach is successful, the growing magnetic field is the eigenvector which eigenvalue becomes positive at the dynamo onset. However, in the subcritical dynamo regime, it is possible to measure the negative eigenvalue of a

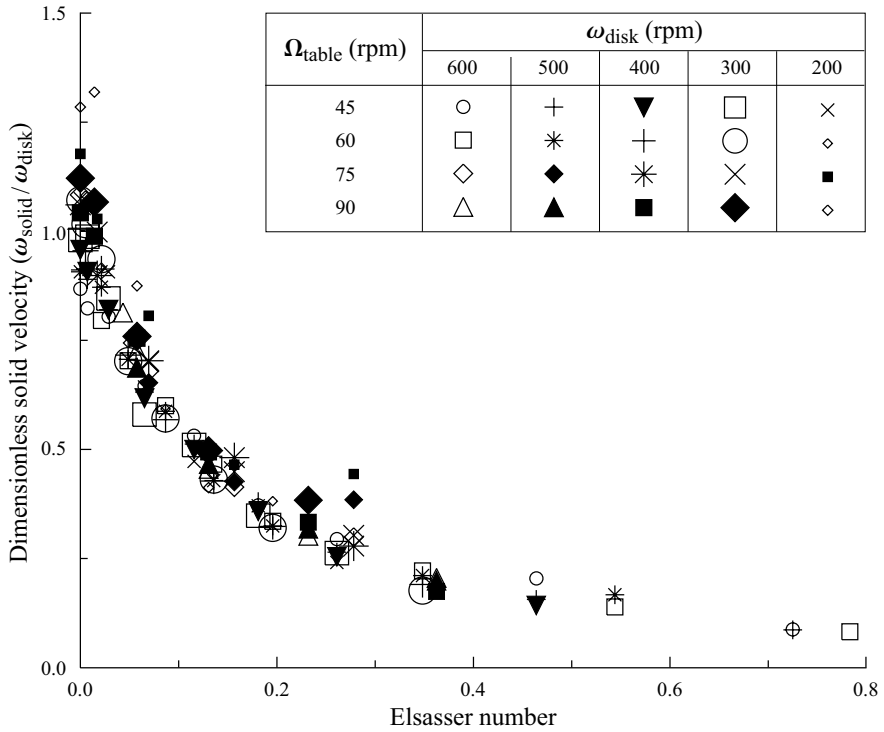

Figure 8.10 - Variation of the angular velocity ω_{solid} of a vortex of liquid gallium over the imposed velocity of the disk ω_{disk} as function of the Elsasser number Λ (see Section 8.2.6). The decrease in amplitude of the angular velocity decreases the amplitude of the induced magnetic field (by ω–effect, see Section 8.3.1). This may be seen as a ω quenching effect (after Brito *et al.*, (1995).

given magnetic field and study its variation as you increase the forcing to get closer to the critical dynamo value. That technique may be a good indicator of the position of the dynamo onset for a given magnetic field.

This technique was first used in the Gailitis *et al.* (1987) group in the Leningrad experiment (see Section 8.2.5). An oscillating magnetic field, close to the eigenvector of the Ponomarenko dynamo, was imposed by a generator and the magnetic response was measured inside the modulus. Figure 8.11 shows that the imposed magnetic field was significatively amplified by the flow and that this amplification was linear in Rm, up to the maximum value of the flow rate tested before the experiment had to be stopped. It may be conjectured that their experiment ended just before the onset of dynamo action.

Alémany *et al.* (2000) have also used this technique to study possible dynamo action in the secondary pump of the fast breeder reactor Superphenix. Extrapolating linearly the growth rate of a decaying magnetic field, they found that the velocity of the pump (500 rpm) was only four times subcritical. We may however slightly moderate their conclusion as there is no theoretical reason to use a linear extrapolation in the kinematic approach (especially far from the onset) to get information on the criticality of the dynamo.

D. Lathrop and collaborators have studied the time relaxation of an imposed magnetic field (Peffley *et al.*, 2000a,b) on the mechanically forced experiment described in Section 8.2.9. For a given flow, they imposed a dipolar magnetic field (either axial $m = 0$ or equatorial $m = 1$) of small amplitude (a few mT) for 1 to $10\,\mathrm{s}$. They turned off the imposed magnetic field and measured the exponential decay. With no motion, the exponential decay is, as expected, the Joule decay time for a sphere. Increasing Rm (Figure 8.12), the decay time increases for $m = 0$ or decreases for $m = 1$. This result disagrees with the kinematic numerical result of Dudley & James (1989) which predict for this type of flow an increase of an equatorial dipole, in agreement with the Cowling theorem (see Chapter 1). This experimental result shows that the nonaxisymmetric part of the flow (due to the propeller, baffles or turbulent fluctuations) plays a significant *rôle* for the generation of the axisymmetric field. The broadwith of the variance of the decay time rates of the magnetic field for large Rm flow is also good indicator of the turbulence in the magnetic field generation process (Peffley *et al.*, 2000a). Note that tests have also been performed with time dependent imposed magnetic field to measure the imaginary part of the eigenvalue.

The experimental kinematic approach which consist to reach the critical eigenvalue of the eigenvector suffers a limitation which is the type of geometry of the magnetic field one can impose on the flow. Although there is almost no time constraint on a kinematic-type dynamo experiment, the geometry of an eigenvector of the magnetic field derived theoretically is reproducible in the laboratory only if it is quite simple. In order to get some kinematic predictions on the onset of the dynamo, water experiments reproducing the same velocity flow as in sodium experiments are broadly

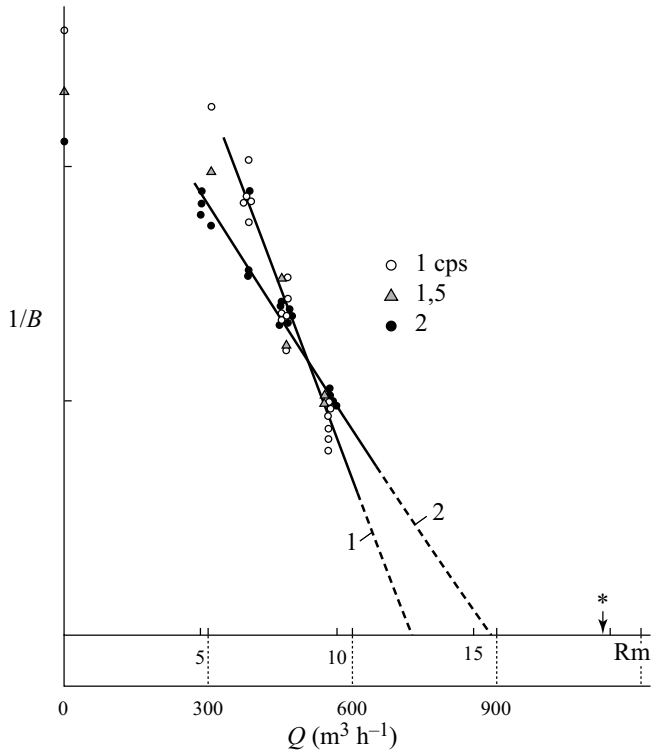

Figure 8.11 - Measureament of the inverse ratio of the induced magnetic field $1/B$ signal versus the flow rates Q (in $\mathrm{m}^3\,\mathrm{h}^{-1}$) for three frequencies of the imposed magnetic field $\mathbf{B}_0$ in the first attempt to run a Ponomarenko experiment in Leningrad (see Section 8.2.5). The linear extrapolation of the experimental results may indicate the critical value of the flux rate for dynamo action. Note that the extrapolation would lead to a critical Rm lower than the theoretical prediction shown with a star around 19 (from Gailitis *et al.*, (1987).

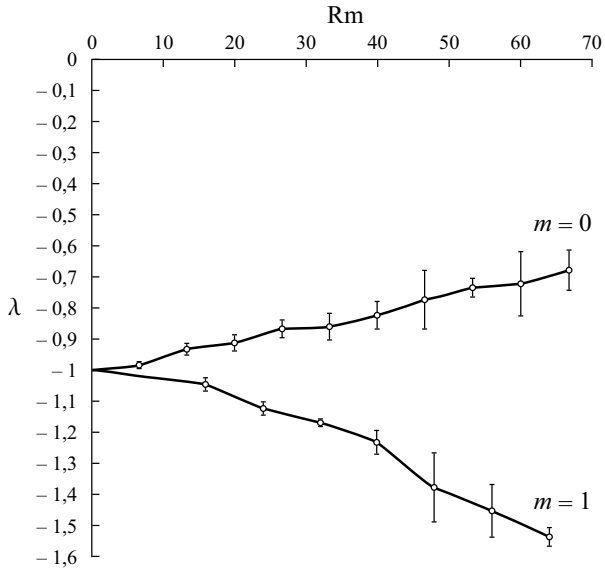

Figure 8.12 - Growth rates (inverse of exponential decay times) λ of an imposed magnetic field after its suppression as a function of magnetic Reynolds number in a College Park experiment (see Section 8.2.9). $m = 0$ refers to an imposed magnetic field aligned with the axis of rotation of the propellers while $m = 1$ to a perpendicular one. The growth rates are normalised by the growth rate at rest. In the numerical model of kinematic dynamo of Dudley & James (1989), the $m = 1$ curve increases instead and crosses the critical axis for a value of Rm around 55 (from Peffley *et al.*, 2000)

performed. In water, velocity measurements are much easier than in sodium, and the averaged flow may be described with a good resolution. Once the experimental velocity field has been measured, it is injected as an input in a computer to solve the kinematic magnetic linear problem. This approach has been followed by many groups; Riga/Dresden group (Stefani *et al.*, 1999), Karlsruhe (Stieglitz & Müller, 2001), VKS group (Marié *et al.*, 2003), Wisconsin (Forest *et al.*, 2002), Perm (Dobler *et al.*, 2003), Grenoble (Schaeffer & Cardin, 2005), Léorat *et al.* (2001).
Numerical kinematic calculations are then used to determine how efficient is an averaged flow to amplify an initial magnetic field and to produce a dynamo. Experimentally, in water, it is quite convenient to change the geometry of the container or the shape of the propellers for example, and check numerically with the new measured velocity fields if you get closer to the dynamo onset. Numerically, it also convenient, once you have the velocity field, to change the boundary conditions of your flow, for example considering insulating or electrical conducting boundaries. This optimisation of velocity flows has successfully worked for the Riga group. Unfortunately, many other groups have shown that tiny difference in the averaged velocity field may change drastically the sign of the eigenvalue (Forest *et al.*, 2003; Marié *et al.*, 2003). Does it mean that dynamo action is not so robust and really depend on very small change in the velocity field? It is also important to note that in this approach, only averaged velocities are considered and that it is may be not sufficient, as fluctuations play an important *rôle* in the dynamics. Another point is that the measured velocity field is only the large scale one, the small scales of the velocity field which may be important to produce an α–effect for example are not measured and not considered numerically.

8.3.6. THE ONSET OF DYNAMO ACTION

Two liquid metals experiments have exhibited a self–induced magnetic field (Gailitis *et al.*, 2000, Müller & Stiegelitz, 2000). Both experiment have been built (see Sections 8.2.7,8.2.8) in order to reproduce well known kinematic dynamos.

THE RIGA DYNAMO

Figure 8.13 shows the measured magnetic field as a function of time for different speeds of the propeller in the Riga dynamo (Gailitis *et al.*, 2000). As expected, the growing magnetic field is a propagating wave along the axis of the experiment (Ponomarenko, 1973). The decay rate and the frequency of the growing magnetic field mode were measured and compared to the predicted one (Figure 8.14). Predictions have been done using a numerical kinematic approach using the averaged

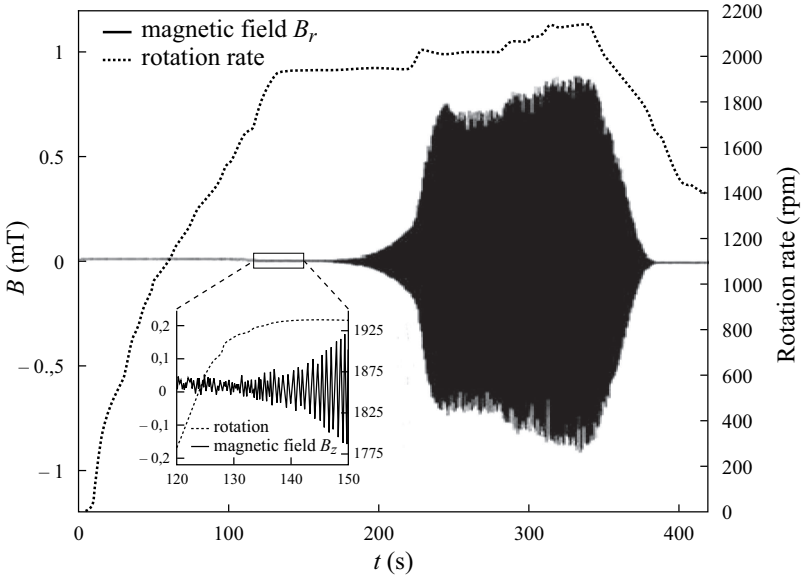

Figure 8.13 - Time evolution of the induced magnetic field (solid line) in the Riga dynamo (see Section 8.2.7). The rotation rate of the propeller is reported (dashed line) and shows the critical rate (around 1925 rpm as shown in the close up), from Gailitis *et al.*, 2002).

velocity field (Stefani *et al.*, 1999; Gailitis *et al.*, 2002). One can note that the onset (within 10% of precision) is correctly described by the numerical approach although the turbulence of the flow (few percents, Gailitis, private communication) is omitted in the central pipe of the experiment. The frequency of the dynamo solution does not seem to be influenced by the saturation of the magnetic field (Figure 8.14). Does it mean that the back reaction is very small in the Riga dynamo? This is still under investigation for the moment. However, measurements of the magnetic field along the axis of the experiment show that the dynamo is mainly produced at the top of the experiment close to the propeller (Gailitis *et al.*, 2001). The onset of dynamo action could also be seen in the evolution of the power dissipated in the experiment as shown in Figure 8.15. Below the onset, the power needed to maintain a rotating rate of the propeller is a cubic power of the rotating rate while there is a clear deviation from that law above the onset (Gailitis *et al.*, 2001).

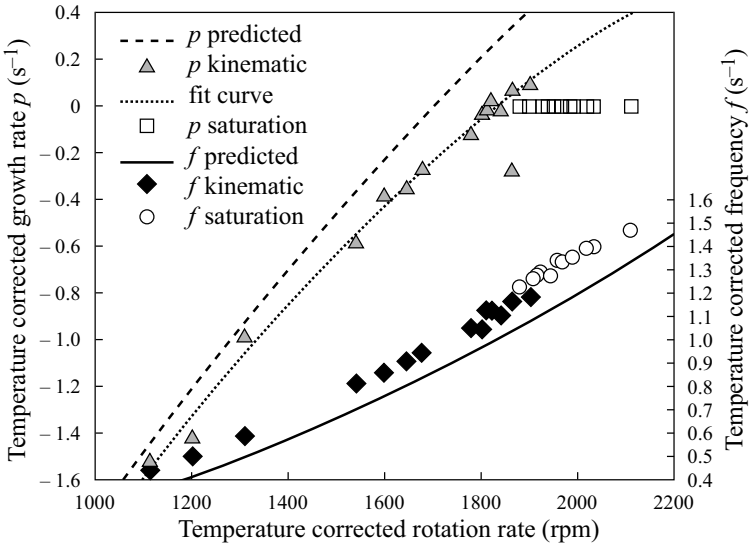

Figure 8.14 - Measurements and predictions of critical growth rates and associated frequency of the magnetic mode for different rotation rates in the Riga dynamo (see Section 8.2.7). Experimental data agrees within 10% with the numerical predictions. Above the onset, the frequency of the saturated magnetic field seems to be equal to the one predicted by the linear theory at the onset (from Gailitis *et al.*, 2002).

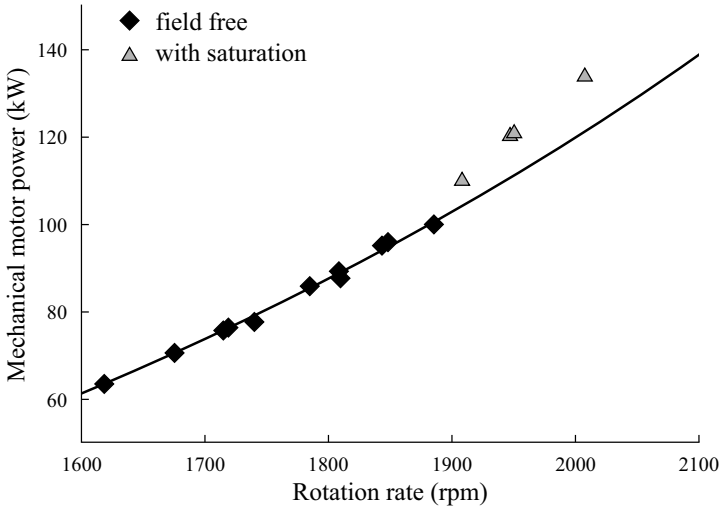

Figure 8.15 - Motor power delivered versus the rotation rate of the propeller in the Riga dynamo (see Section 8.2.7). Below the onset, the dissipation increases as the cubic power (solid line) of the rotation rate. Extra power is needed to maintain the rotation rate above the dynamo onset which gives an evaluation of the power needed to sustain the dynamo state (from Gailitis *et al.*, 2001).

THE KARLSRUHE DYNAMO

A self–induced magnetic field was observed in the Karlsruhe experiment (Stieglitz & Müller, 2001) for imposed flow rates $Q_{\rm sodium}$ (see Section 8.2.8) comparable to the predicted onsets (Figure 8.16), the exact experimental onset being lower than the one predicted by Rädler *et al.* (1998) and by Tilgner (1997) by only 10%. However, the numerical predictions have strongly modeled the fluid flow of the experiment (only the straight part of the tubes have been included in the modelisation for example). The measurements of the induced magnetic field, as well as the pressure drop in the piping system, seems to show a smooth rather than a sharp Hopf bifurcation (Müller *et al.*, 2004). Before the onset, the measured induced magnetic field may be understood as the amplification (by a factor 10) of the Earth's magnetic field as a kinematic effect (see Section 8.3.5). Typical growth rates of $10\,{\rm s}^{-1}$ could be deduced from Stieglitz *et al.* (2001) during the transient after the onset; these are ten times greater than the ones predicted by Tilgner in 1997. Nevertheless, the spatial distribution of the experimental saturated magnetic field (Stieglitz & Müller, 2002) is in agreement with the one predicted by the two numerical studies (Tilgner, 1997; Rädler *et al.*, 2002). The growing magnetic field in the Karlsruhe experiment varies however with the initial external imposed magnetic field and may change its

sign depending on initial conditions (Müller *et al.*, 2004). This behaviour was also reproduced numerically by Tilgner & Busse (2002).
Like in Riga, the Karlsruhe dynamo numerical modelisation remarkably agrees with the prediction of the kinematic or mean field approach. The mean field approach can be seen as very successful in the Karlsruhe dynamo experiment but that could be expected as the experiment has been built to be a two-scale dynamo, suitable to the mean field approach: the velocity field is small scale (size of the helicoidal tube) whereas the magnetic field is dominated by the large scale (size of the dynamo modulus). The Karlsruhe experiment may be seen as an experimental proof of the validity of the mean field theory in MHD.

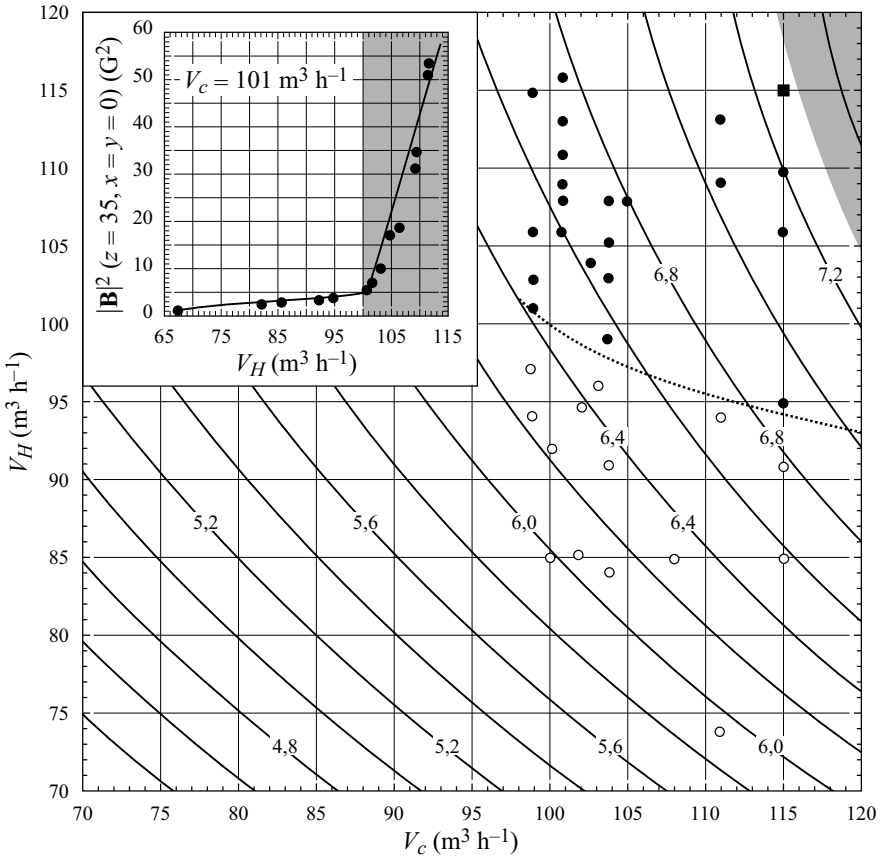

Figure 8.16 - Phase diagram of the Karlsruhe dynamo (see Section 8.2.8). V_C and V_H (in m^3/h) are the flow rates in the central pipes and in the helicoidal pipes respectively. Open circles (○) are non dynamo states while full circles (●) are dynamo states. A dashed line separates those. In the upper corner, one sees the evolution of magnetic energy ($|\mathbf{B}|^2$) against the helicoidal flux V_H for a constant V_C. The linear fit of the data above and below the onset determines very precisely the value of the onset. Mean field theory predictions of the dynamo state are shown in grey (upper right corner) and a typical onset determined by the numerical kinematic approach appears as a filled square (from Stieglitz & Müller, 2001).

8.3.7. THE EFFECT OF TURBULENCE

Laminar description of the velocity flow has enabled a good prediction of the onsets in both successful dynamo experiments. Nevertheless, these flows have to be turbulent as seen in the introduction with the computation of typical Re. It is not simple to understand why turbulence is not changing the onset of dynamo action.
For smaller experiments, the kinematic numerical studies devoted to predict the onset of dynamo action with the averaged large scale flow field have predicted possible dynamos in the parameter regime where were run experiments, but dynamos were never observed (Peffley *et al.*, 2000; Bourgoin *et al.*, 2002). One may say that it is because the averaged flow numerically used for kinematic computations is unlikely to happen during the real experiment, however that worked for Riga and Karlsruhe dynamos. One may also think that it is because the characteristic turbulent time is much smaller than the exponential growth rate of the dynamo. It is known indeed from kinematic dynamo studies that only small changes in the velocity field may strongly change the growth rate of the magnetic field. If a turbulent experiment could therefore exhibit a favorable dynamo flow for a certain time, it may not last long enough to start a dynamo.
Sisan *et al.* (2003) in the College Park's experiment (see Section 8.2.9) have clearly identified the effect of an imposed magnetic field on the dynamic regime of their experiment. For a given Rm (7.5), they varied the intensity of the imposed magnetic field. As the interaction parameter N increases, the measured induced magnetic field shows different time and amplitude variations which may reveal different magneto-turbulent regimes. Five distinct characteristic induced magnetic field were identified in Figure 8.17.

On the edge of the context of experimental dynamos, experiments of MHD turbulence have been built to study fundamental properties of the flow (dedicated to metallurgy), see Moreau (1998). In general terms, the presence of a strong magnetic field tends to form quasi-two-dimensional flows aligned with the magnetic field (Moreau, 1990) which can exhibit 2D turbulent properties (Alémany *et al.*, 1979). A recent experimental study of this type of MHD turbulence has been carried out by Messadek & Moreau (2002) on instable shear flows at low Rm. The MHD turbulence enlarges the thickness of the shear zone by two orders of magnitude which enhances the momentum transport and the mixing across the layer. As in many other experimental studies, the turbulence of the flow is characterised by the measurements of magnetic and kinetic spectra.

8.3.8. SPECTRA

Theories of turbulence generally predict the behaviour of scalar fields in a fluid flow in term of spectral decomposition. Although these spectra are generally in the spa-

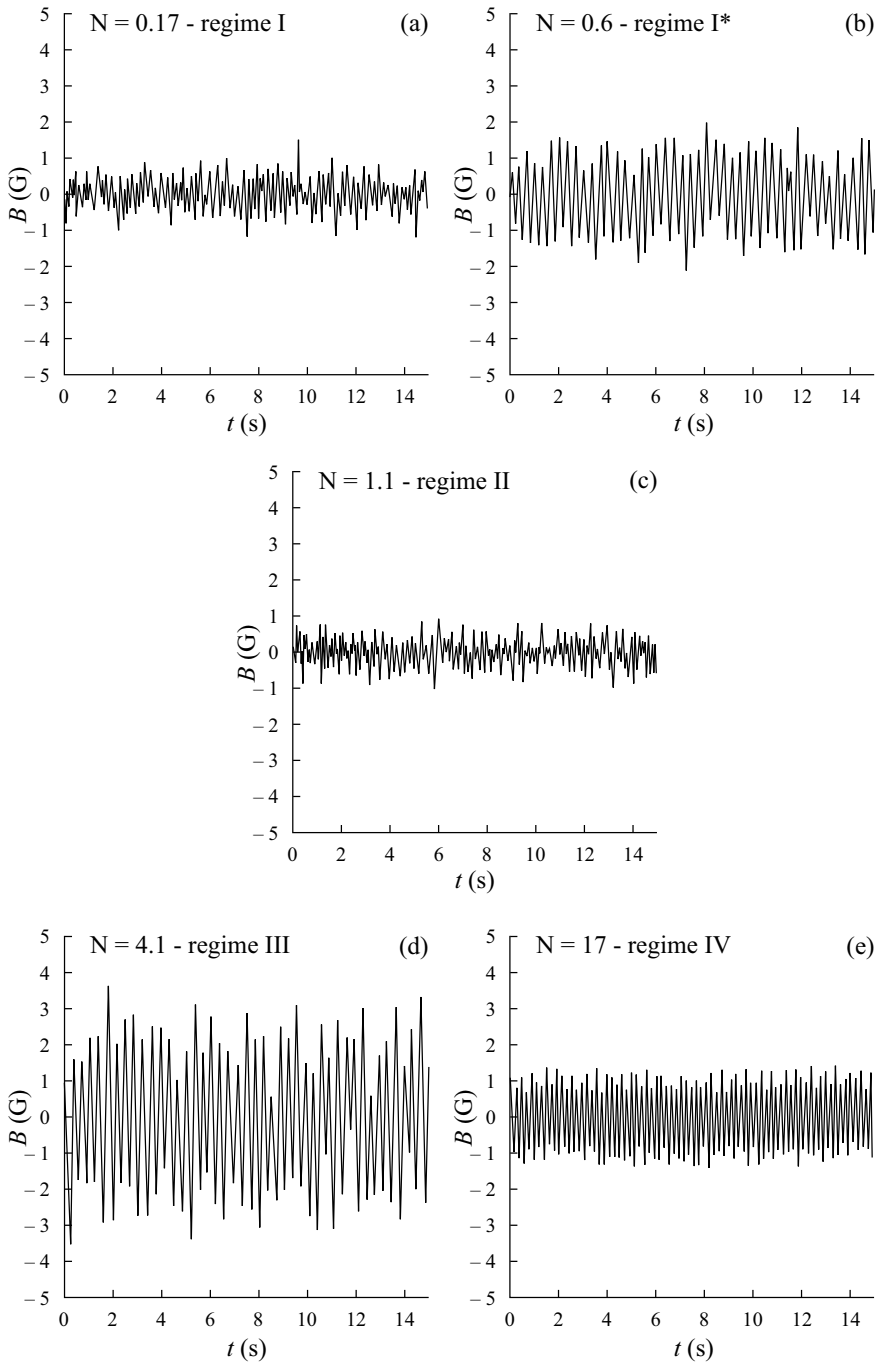

Figure 8.17 - Time evolution of the induced magnetic field B for different interaction parameter N in the mechanically forced experiment in College Park (see Section 8.2.9). The rotation rate of the propellers is fixed ($\mathrm{Rm} = 7.5$). Different regimes may be identified looking at the frequency and amplitude of the measured magnetic field, from Sisan *et al.*, 2003).

tial domain, it is not convenient to measure the spatial distribution of a field during experiments. Instead, time variations of theses fields are measured, the Taylor (or ergodicity) hypothesis connecting time and spectral variations for homogeneous turbulence (Frisch, 1995; Lesieur, 1997).

Kinetic energy spectra are generally deduced from pressure measurements while magnetic energy spectra come from the measurement of a component of the magnetic field. In presence of an external magnetic field and with a low Rm flow, the dependence between the two spectra proceeds from the induction equation. If you suppose the kinetic energy $E_k \propto k^\alpha$ (k is the wavenumber and $\alpha < 1$), using the induction equation, one can show that the magnetic energy vary as $E_m \propto k^{\alpha-2}$ (Moffatt, 1978; Moreau, 1990).

Depending on the intensity of the imposed magnetic field measured by the interaction parameter N, we may have two types of spectra dependence. For low N, the turbulence is of Kolmogorov type with $E_k \propto k^{-5/3}$ and $E_m \propto k^{-11/3}$. This has been seen in many experiments. The VKS group (Odier *et al.*, 1998; Bourgoin *et al.*, 2002) have documented this regime where the magnetic field behaves as a passive vector. In Figure 8.18, magnetic measurements show a clear $-11/3$ power law above the frequency of the driving disk while the authors proposed an hyperbolic range of frequencies for the fluctuations of the induced magnetic field below it. Although such a k^{-1} behaviour is also reported in the Karlsruhe experiment (Müller *et al.*, 2004) and in the Maryland experiment (D. Lathrop, private communication), it is not clear to understand the physical mechanism which leads to such a power law.

For strong magnetic field (high N), Alémany *et al.* (1979) found $E_k \propto k^{-3}$ and $E_m \propto k^{-5}$ in an experiment where the turbulence was produced by the motion of a grid and the velocity were measured using quartz-coated hot film probes. As shown by the spectrum dependence, the Joule effect strongly influences the rate of dissipation of energy and leads to an anisotropic flow during the decay of the turbulence. The -3 exponent of the kinetic energy may be deduced from the balance between angular transfer time and Joule dissipation time. A second experiment has been performed to study this regime, under stationary forcing this time. Messadek & Moreau (2002) found the $-5/3$ exponent for the spectral kinetic energy at low N and -3 exponent at high N.

Under a dynamo state, power spectral density of the magnetic field have been measured in the Karlruhe experiment (Stieglitz *et al.*, 2002, Müller *et al.*, 2004). Figure 8.19 shows typical spectra of the induced magnetic field inside the modulus (see Section 8.2.8). Above the critical flow rate (around $V_C \simeq 120\,\mathrm{m^3\,h^{-1}}$), a self–induced magnetic field is generated and a peak appears in the magnetic spectrum around 1 Hz. One would like to interpret the frequency of this peak as the injecting magnetic energy scale using the ergodicity hypothetis. However, the frequency associated to the helicoidal flow may be evaluated to 5 Hz. This value is too large by at least a factor 2 to explain the power peak. Moreover, the frequency of the power

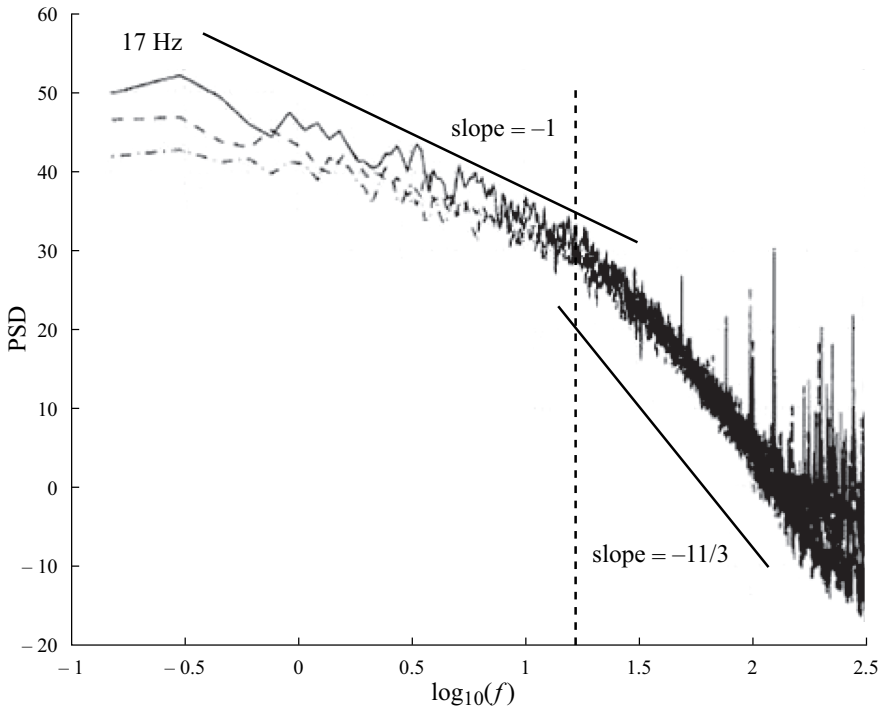

Figure 8.18 - Power spectral density function of the induced magnetic field in the VKS experiment (see Section 8.2.10). Above the frequency (dashed line) associated to the rotating rate of the propeller, the spectra is in agreement with the Kolmogorov prediction (low N). Below this frequency, the spectra is hyperbolic, from Bourgoin *et al.*, 2002).

peak changes with the supercriticality of the dynamo and not with the volumetric rate of the helicoidal tube. Note that Müller *et al.* (2004) proposed an interpretation in term of Alfvén waves traveling along the cylinders. For larger frequencies (above the peak), the Joule dumping of the magnetic field leads to a large negative exponent in the power spectrum (from -3 to -5, and sometimes even smaller). The -5 exponent is in agreement with the results of Alémany *et al.* (1979). For smaller frequencies (below the peak), they found a f^{-1} type behaviour like in Bourgoin *et al.* (2002) study. In the context of their dynamo, they link this observation to the prediction of Pouquet *et al.* (1976) based on theoretical arguments of inverse cascade of magnetic helicity.
Experimental spectra at large Rm are always difficult to interpret. It is difficult to get a clear power law for a decade in frequency and inferring an exponent without any theoretical background is rather conjectural. As already mentionned, conversion from temporal to spatial field are based on the ergodicity hypothesis which remains an hypothesis in MHD flows. Furthermore, theories are generally done for $\mathrm{Pm} = 1$ (Biskamp, 1993) and the compatibility of theoreticals predictions with with liquid metal experiments is not straightforward.

8.3.9. THE β–EFFECT AND TURBULENT VISCOSITY

The β–effect is a turbulent effect associated to the $\boldsymbol{\nabla} \times (\mathbf{u} \times \mathbf{B})$ in the induction equation and can be modeled as a magnetic dissipative effect. In some regimes, the β–effect could modify the molecular magnetic diffusivity $\eta = 1/\mu_0\,\sigma$ of conducting fluids. Reighard & Brown (2001) has measured the apparent magnetic diffusivity of sodium as a function of the Rm. They found a reduction from the molecular value of the electrical conductivity of 4% at Rm of order 10 . No such effect has ever been measured in other sodium experiments. Nevertheless, the mean field theory developed by Rädler *et al.* (2002) evaluated a β–effect between 1 to 10% of the molecular value in the Karlsruhe dynamo flow. The good agreement between the mean field approach and the experimental results may be interpreted an indirect observation of the β–effect. Moreover, Tilgner & Busse (2002) with their kinematic approach, need to increase the magnetic diffusivity in order to explain correctly the precise position of the onset of the Karlsruhe dynamo. In that case, they associate the enhanced magnetic diffusivity to the averaged diffusivity of sodium and stainless steel instead of a turbulent effect.
Similarly, the non-linear term in velocity in the momentum equation may be modeled as a dissipative viscous effect. The turbulent viscosity (and more sophisticated models) is largely used in geophysical and astrophysical numerical fluid dynamics (meteorological or oceanographic models for example). Direct experimental measurements of the turbulent viscosity are quite difficult in particular because very precise maps of the velocity field are required within the bulk of the flow. Lathrop *et*

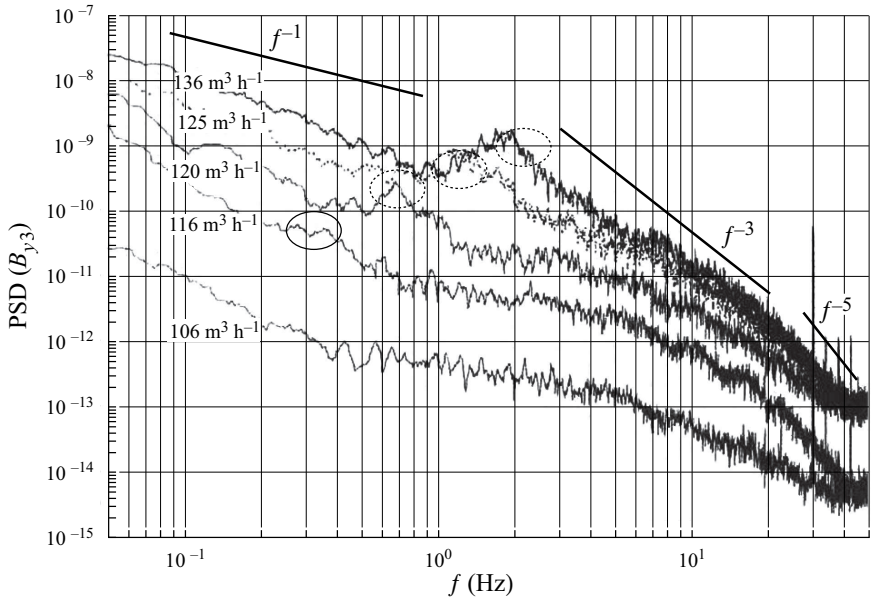

Figure 8.19 - Power spectral density of a component of the magnetic field (perpendicular to the axis of the tubes at the center of the modulus) in the Karlsruhe dynamo modulus (see Section 8.2.8). The helicoidal flux rates are set to $100\,\mathrm{m^3\,h^{-1}}$ and the central flux rate is increased from 106 to $136\,\mathrm{m^3\,h^{-1}}$, the onset of the dynamo occuring around $120\,\mathrm{m^3\,h^{-1}}$. A central peak appears above the onset, separating the spectra in two parts: an hyperbolic range for low frequency and a steeper exponent (-3 to -5) for higher frequency, from Müller *et al.*, 2002).

al. (1992) in a Couette experiment have interpreted the measured torque delivered by the rotating motor in term of turbulent viscosity and proposed a law for the turbulent viscosity as a function of Re, the hydrodynamic Reynolds number. More recently, Brito *et al.* (2004) have shown experimental evidences of turbulent viscosity in the context of a rotating flow.

8.3.10. SATURATION OF THE DYNAMO

The two successful experimental dynamos exhibited a saturated state of the self–sustained magnetic field after a period of exponential growth (see that exponential growth in Figure 8.13 for example, in the Riga dynamo). In both experiments, the injected mechanical power required to drive the flow was measured as a function of the averaged velocity of the fluid flow. Figure 8.15 shows an increase of around $10\,\mathrm{kW}$ after the onset of the dynamo regime in the Riga experiment. If one consider that this increase of power was directly dissipated by Joule effect, one can find a typical length scale of dissipation:

$$P_j \propto \frac{B^2 L^3}{\mu_0^2 \sigma L_d^2} = 10^4\,\mathrm{W} \Rightarrow L_d \propto 10^{-3}\,\mathrm{m}\,.$$

for $B = 1\,\mathrm{mT}$, $L = 1\,\mathrm{m}$. This Joule dissipation scale is much larger than the viscous dissipation scale ($L_d \propto 10^{-6}\,\mathrm{m}$ if we consider $\mathrm{Re} = 1$ with $U = 1\,\mathrm{m\,s^{-1}}$) and may be the main dissipative process in the dynamo state. At the dissipation scale, Rm is small and the results of turbulence at low Rm should apply, particularly the spectrum dependence in k^{-3} for the kinetic energy (see Section 8.3.8). Figure 8.19 shows indeed a steep tail of the spectra (for large frequencies) which may be the signature of the low Rm turbulence.

The balance between the non linear velocity term and the Lorentz force may lead to the prediction of the intensity of the saturated magnetic field. Pétrélis & Fauve (2001) and Tilgner & Busse (2002) had to introduce a turbulent viscosity (at least 10^4 times the molecular one) to explain the observed value of the saturated magnetic field in Karlsruhe and Riga. Their approach excludes any laminar viscous balance which would lead to an intensity of the saturated magnetic field too low compared to the experimental measured one.

The saturation mechanism may be also associated to a real change in the fluid flow dynamics after the onset of the dynamo. In Riga, observations of the saturated magnetic field show indeed a dependence along the height of the experiment (Gailitis *et al.*, 2001) and sodium originally at rest (at the edge of the modulus, see Section 8.2.7) is driven into motion after the onset (Gailitis, private communication). The same idea was proposed by Tilgner & Busse (2001) for the Karlsruhe experiment with the presence of vortices of sodium in between the tube of the modulus (see Section 8.2.8).

8.4. CONCLUSION

Two experimental dynamos (Gailitis *et al.*, 2000; Müller & Stieglitz, 2000) have been observed in the laboratory. They demonstrated experimentally the existence of a dynamo regime where the magnetic field is self–sustained in a fluid flow where the dynamo was predicted theoretically. These two experiments have shown that the dynamo action occured where the analytical and numerical methods predicted it, even if the experiment could not exactly reproduce the idealised world of models (boundary conditions, presence of stainless steel, small scale flow, turbulence). These two success are really associated to the choice of very robust flows to produce the dynamo action. In the dynamo state, these two experiments exhibit results (power, spectra, ...) which are not fully understood yet and many questions arise regarding the presence of a large magnetic field. A more homogeneous experiment, perhaps, would answer more easily these questions.
Surprisingly, for more homogeneous experiments, the dynamo onset seems to vary a lot with small variations in the velocity field as already mentionned; we can conclude that the robustness of these flows to produce a self–sustained magnetic field is weaker. Lathrop and collaborators tried different configurations to look for a possible dynamo with their experimental set-up. Shew *et al.* (2001) report on tests with change of propellers, addition of cupper rings or plates at the equator, change of baffles in the sodium tank. A clear variation in the exponential decay times of the imposed magnetic fields associated to these changes is observed but it is difficult to infer general properties on dynamo mechanism from these tests. Shew *et al.* (2002) built an updated version of the Lowes & Wilkinson dynamo, where the external solid housing is replaced by liquid sodium. No dynamo has been observed in this configuration. The VKS group also changed the electrical boundary conditions of their vessel adding a copper housing without observing the dynamo (Bourgoin *et al.*, 2002), although a numerical kinematic study predicted a reduction by a factor 2 of the critical Rm when the boundaries were changed from insulating to perfectly conducting (Marié *et al.*, 2002). Note that Martin *et al.* (2000) and Frick *et al.* (2002) have tried to increase the magnetic permeability of the liquid metal by the use of ferromagnetic iron beads or samll particles. Frick *et al.* (2002) proposed a linear law for low concentration of small particles (0.01 to $0.1\,\mathrm{mm}$ of diameter) which may increase the magnetic Reynolds number by a factor two.
Building-up a dynamo experiment is a very long and hard enterprise, that is why most of the present dynamo experiments or projects presented throughout this survey intend to observe a dynamo effect in their homogeneous fluid flow experiment in the near future. Among all the working groups we may forecast that two of them will soon observe dynamo action: The VKS group is planning to run a second version of their Von Kàrmàn experiment in a larger container, with new optimised propellers and a cooling system unit. The College park group is building a very large rotating

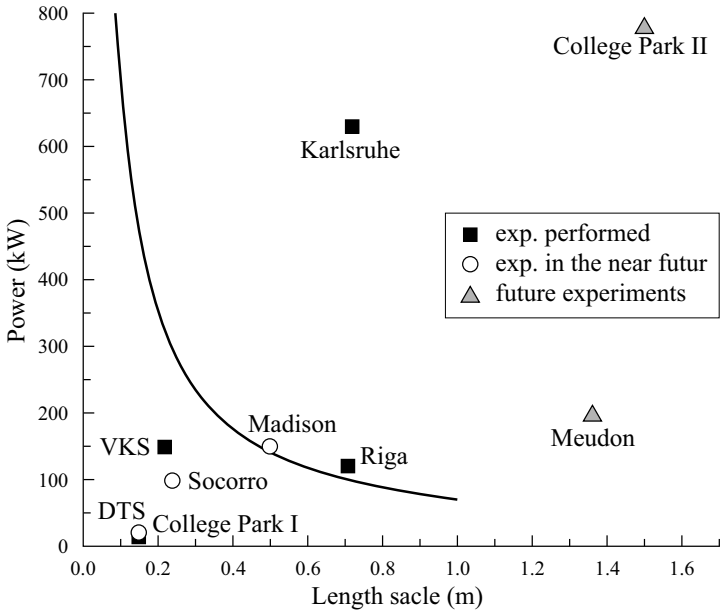

Figure 8.20 - Summary of the presents experiments and projects presented in term of caracteristic length scale (X-axis) versus the mechanical power (in kW) injected to run the sodium flow. Triangles: possible future experiments; Circles: experiments to be run in the near future; Squares: experiments already performed. The curve is an imaginary line that may separate the successfull vs the non-dynamo experiments.

spherical experiment with 15 tons of sodium which should have all the ingredients to self–sustain a magnetic field if we dare to compare it with natural planetary dynamos.

Size and power are the two main factors which determine the cost of an experiment. Small experiments are easier to build and to change. But up to now, only large experiments have been able to self–induce a magnetic field in liquid sodium. Clearly, in order to reach a given magnetic Reynolds number, you have to choose a trade-off between the typical scale of the flow and the typical velocity (and consequently the power). Too much power injected in a small experiment may end with cooling problems. On the contrary, large experiments need a lot of power to reach high velocities of the fluid flow. Nataf (2003) produced three years ago an interesting representation of the power versus size of dynamo experiments. We show an updated version of this representation in Figure 8.20 including the new projects. Note however that this graph does not take into account the type of flow generated into the vessel which is may be a crucial point when the vigour of the flow is close to start a dynamo.

The understanding of MHD turbulence is the main challenge for our community in the next period. Studies of spectra are precious and enable a classification of dif-

ferent regimes. As noted in Section 8.3.8, experimental data are generally measured as a function of time and we rely on the ergodicity hypotheshis to interpret these spectra in term of spatial behaviour of the MHD turbulence. Theories with very low Prandtl numbers will be needed to help the interpretation of liquid sodium experiments.

Global rotation could be a key ingredient for dynamo action. The presence of rotation favours a direction in the flow and the isotropic turbulence shifts to a quasi geostrophic turbulence. This is the case also with precessional flows where Gans (1970) has observed a large amplification of the magnetic field, still unexplained. Quasi-geostrophic dynamos have just been computed based on shear flows taking into account the properties of a rapidly rotating flow (Schaeffer & Cardin, 2006). These preliminary results are encouraging for experimental dynamo modeling of rotating planets (low Pm, low E) because they exhibit robust dynamos which can be understood as $\alpha\omega$ dynamos. Does the rotation increase the robustness and the ability of the flow to produce the dynamo action?